




## Allowed $\beta^-$ decay of bare atoms with $A \approx 60-80$ in stellar environments

Arkabrata Gupta <sup>1</sup>, Chirashree Lahiri <sup>2</sup>, and S. Sarkar <sup>1,\*</sup>

<sup>1</sup>*Department of Physics, Indian Institute of Engineering Science and Technology, Shibpur, Howrah 711103, India*

<sup>2</sup>*Department of Physics, Surendranath Evening College, 24/2 M. G. Road, Kolkata 700009, India*



(Received 27 August 2022; revised 5 May 2023; accepted 15 June 2023; published 24 July 2023)

We have calculated  $\beta^-$  decay rates to the continuum and bound states of some fully ionized atoms in the stellar  $s$ -process environment having free electron density and temperature in the range  $n_e = 10^{26}-10^{27} \text{ cm}^{-3}$  and  $T = 1 \times 10^8$  to  $5 \times 10^8 \text{ K}$ , respectively. The presence of bare atoms in these particular situations has been confirmed by solving the Saha ionization equation taking into account the ionization potential depression (IPD). At these temperatures, low lying excited energy levels of parent nuclei may have thermal equilibrium population and those excited levels may also decay via  $\beta^-$  emission. The nuclear matrix element (NME) of all the transitions of the set of 15 nuclei is calculated using nuclear shell model. These NMEs are then used to calculate the comparative half-life ( $ft_{1/2}$ ) of the transitions. Calculated terrestrial half-lives of the  $\beta^-$  decays are in good agreement with the experimental results in most of the cases. Decay to bound and continuum states of bare atoms from ground and/or isomeric levels and excited nuclear levels are calculated separately. The ratio of bound state to continuum state decay rates as a function of IPD modified  $Q$  value reveals that the bound state  $\beta^-$  decay rate may compete and even dominate for  $Q$  value  $< 100 \text{ keV}$ . The importance of the bound state  $\beta^-$  decay in stellar situations has been shown explicitly. We have calculated total  $\beta^-$  decay rates (bound state plus continuum state) taking into account the IPD corrected neutral atom  $Q$  value as a function of density and temperature. We have also presented results for the stellar  $\beta^-$  half-lives and compared the ratio of neutral atom to bare atom half-lives for different density and temperature combinations. These results may be useful for  $s$ -process nucleosynthesis calculations.

DOI: [10.1103/PhysRevC.108.015805](https://doi.org/10.1103/PhysRevC.108.015805)

### I. INTRODUCTION

$\beta^-$  decay is a weak interaction process that allows the conversion of a neutron into a proton with the creation of an electron and an antineutrino in the continuum state. Terrestrial  $\beta^-$  decay has been studied through the decades both experimentally and theoretically since its discovery, which enriched the knowledge of nuclear interaction processes and nuclear structure. The terrestrial  $\beta^-$  decay of an atomic nucleus occurs from the nuclear ground state and isomeric states. However, the scenario differs when parent and daughter atoms are in a stellar environment. It is possible even for the high- $Z$  ( $\approx 35$ ) elements to be partially or fully ionized, due to high temperature ( $\approx 10^8 \text{ K}$ ), wherein free electron density also plays a role [1]. This creates vacancy in atomic orbits. Also, the environmental condition leads to depression of the ionization potential which in turn not only changes the  $Q$  value of  $\beta^-$  transitions but also affects the charge state distribution of the atoms. Availability of vacancy, i.e., free phase space in the atomic orbits may lead to another type of  $\beta^-$  decay, known as bound state  $\beta^-$  decay. In 1947, Daudel *et al.* [2] first theoretically predicted this new branch of  $\beta^-$  decay as the phenomenon of the creation of an electron in the empty bound atomic orbit. This is just the time reversed process of atomic

orbital electron capture. Later, in the early 1960s, Bahcall used renormalized V-A theory to calculate the bound state  $\beta^-$  decay rate [3]. After many years, in the 1980s Takahashi *et al.* [4,5] made more elaborate studies of the bound state  $\beta^-$  decay in the context of nuclear astrophysics. The study of bound state decay has also become relevant in other contexts, such as in the study of atomic effects on  $\beta^-$  decay [6,7]. Takahashi and Yokoi [4] calculated  $\beta^-$  decay rates including bound state  $\beta^-$  decay of a number of nuclei relevant for the  $s$  processes. Takahashi and co-workers [8] also predicted a way to observe this phenomenon in a terrestrial laboratory. In the following decade, Jung *et al.* [9] first succeeded in experimentally observing this phenomenon in the case of the  $^{163}\text{Dy}$  atom by storing the fully ionized parent atom in a heavy ion storage ring. After that, Bosch *et al.* [10] studied the bound state  $\beta^-$  decay for bare  $^{187}\text{Re}$  which was helpful for the calibration of a  $^{187}\text{Re} - ^{187}\text{Os}$  galactic chronometer [11]. Further experiment with bare  $^{207}\text{Tl}$  [12] showed the simultaneous measurement of bound and continuum state  $\beta^-$  decay rate. Experimental study of bound state  $\beta^-$  decay of  $^{205}\text{Tl}^{81+}$  ions also was done recently [13,14]. However, to study the role of this phenomenon in the context of stellar processes, such as nucleosynthesis, one has to rely only on the theoretical predictions of the  $\beta^-$  decay rates that include both bound and continuum state decays.

We could not trace in the literature any further theoretical study on bound state  $\beta^-$  decay in the context of nuclear

\*Corresponding author: [ss@physics.iests.ac.in](mailto:ss@physics.iests.ac.in)

astrophysics after the works of Takahashi and Yokoi [5]. With the availability of more accurate modern day experimental  $\beta^-$  decay half-lives, branching, and energetics, we studied both the bound state and the continuum state  $\beta^-$  decay from the ground state and isomeric states of the parent nuclei in 2019 [15]. In that study, we showed the maximum possible  $\beta^-$  decay rate of bare atoms in the mass range  $A = 60-240$ . Apart from this, we examined the case studies as mentioned in the work of Takahashi and Yokoi [5]. We also showed for the first time that for some nuclei, it is possible that the  $\beta^-$  branching may flip [15] in comparison to the terrestrially measured branching, if the contribution from bound state  $\beta^-$  decay is taken into account. It was shown [4,15] that bound state  $\beta^-$  decay is possible for the transitions which have low and negative  $Q$  values if the binding energy of the atomic shell is large enough to make the  $Q$  value positive. Following this, recently Liu *et al.* [16,17] also studied bound state  $\beta^-$  half-lives for bare atoms.

Terrestrially, as mentioned above, only the ground state and a few of the isomeric levels decay via  $\beta^-$  emission. However, in proper stellar environments, there is a definite probability of thermal equilibrium population of higher excited nuclear levels. In that case  $\beta^-$  decay from those levels may come into play, if allowed by the energetics and  $\beta^-$  decay selection rules.

In an earlier attempt, we reported [18] the calculated total  $\beta^-$  decay rates of an atom in its bare form to the bound and continuum states for the  $s$ -process situation using only experimentally available  $ft_{1/2}$  (comparative half-life, commonly termed as  $ft$ ) values.

In the present attempt, we calculate both bound and continuum state  $\beta^-$  decay for some fully ionized atoms in the mass range  $A = 59-81$  in a stellar environment assumed to exist during the  $s$ -process. For example, one may consider [4] that the environment mainly consists of 75% bare H,  $\approx 25\%$  bare He, and traces of heavy ions floating in the ionized sea of H and He. Temperature ( $T$ ) and free electron number density ( $n_e$ ) of the environment were chosen, following Takahashi and Yokoi [4], in the range  $T = 1 \times 10^8$  to  $5 \times 10^8$  K and  $n_e = 10^{26}-10^{27}$  cm $^{-3}$ , respectively. Experimental  $\beta^-$  decay half-life and branching for transitions from the ground state and isomeric states in these nuclei are available [19] presently. Consequently, the experimental values of the comparative half-life for these transitions are available. However, the comparative half-lives corresponding to the  $\beta^-$  transitions from the nuclear excited levels are not available, since these decays do not occur terrestrially.

In their work, Takahashi and Yokoi [4,5] had taken the contribution of the  $\beta^-$  decay rate from the nuclear excited states to calculate the total  $\beta^-$  decay rate of the parent nuclei. However, to calculate the decay rate from these nuclear excited states, they estimated the comparative half-lives in different ways. For example, in some cases, they adopted average  $ft$  values from older systematic studies, and even in some cases they had used a single  $ft$  value for all transitions from a parent level. In this work, we evaluated the  $ft$  values for relevant allowed  $\beta^-$  transitions for all nuclei in the range by realistic nuclear shell-model calculations.

In this paper, we present bound and continuum state  $\beta^-$  decay rates separately to reveal the importance of the former rate for stellar evolution processes.

To confirm the presence of bare atoms, the Saha ionization equation has been solved. The required ionization potential [20] was modified using ionization potential depression (IPD). IPD was estimated using the fitted formula of Takahashi and Yokoi [4] which was based on Stewart-Pyatt model [21] to account for environmental conditions.

The paper is organized as follows: Section II contains the methodology of our entire calculation for  $\log ft$  and bare atom  $\beta^-$  decay rates. In Sec. III A, we discuss shell-model calculation of  $ft$  values. Section III B contains a discussion about the availability of bare atoms in different stellar environments, variation of decay rates with temperature and density, variation of bound to continuum decay rate ratio, and total  $\beta^-$  decay rates in detail. Also, in this section, we present the change in  $\beta^-$  half-life in a stellar environment in comparison with terrestrial half-life. In Sec. IV the conclusion of this work is discussed. Later, in Appendix A we discuss briefly the procedure to choose the model space and Hamiltonian for calculation of  $\log ft$  using the nuclear shell model. The method to find the GT quenching factor is discussed in Appendix B, and the Saha ionization equation in Appendix C.

## II. METHODOLOGY

### A. $\beta^-$ decay rate

In this work, we have dealt with the allowed  $\beta^-$  transitions of some nuclei involved in the  $s$  process in the mass range  $A = 59-81$ . The contributions of forbidden transitions, though not many in number, are negligible in the determination of the  $\beta^-$  decay rate for these nuclei and thus we have not taken those forbidden transitions into account. The experimental  $\log ft$  values for the allowed transitions range from 4.26 to 8.72, whereas the experimental  $\log ft$  values for the first forbidden  $\beta^-$  transitions are in the range 9.80–11.14. The nuclei in this range, which have sizable contribution from nonunique or unique forbidden transitions, are not taken in the present study.

The transition rate (in s $^{-1}$ ) for an allowed ( $a$ ) transition ( $Z-1 \rightarrow Z$ ) is given by [4]

$$\lambda = [(\ln 2)/ft](f_a^*). \quad (1)$$

Here  $t$  is the partial half-life of the specific  $\beta^-$  transition and  $f_a^*$  is the lepton phase volume part for allowed decays described below. The  $ft$  values have been obtained via shell-model calculations.

The lepton phase volume  $f_a^*$  [4] for the continuum state  $\beta^-$  decay can be expressed as

$$\begin{aligned} f_a^*(\text{Continuum}) &= \int_1^{W_c} \sqrt{(W^2 - 1)} W (W_c - W)^2 F_0(Z, W) \\ &\quad \times L_0(1 - f_{FD}(\eta, \beta)) dW, \end{aligned} \quad (2)$$

with

$$f_{FD}(\eta, \beta) = \frac{1}{1 + \exp(\beta(W - 1) - \eta)}. \quad (3)$$

Here the factor  $(1 - f_{FD}(\eta, \beta))$  is taking care of Pauli's exclusion principle,  $W_c = Q_c/m_e c^2 + 1$  is the maximum energy

available to the emitted  $\beta^-$  particle,  $\beta = m_e c^2 / k_B T$ , and  $\eta$  is the electron degeneracy parameter (i.e., chemical potential without the rest mass divided by  $k_B T$ ) and can be obtained from the electron number density  $n_e$ , where

$$n_e = \int_1^\infty W \sqrt{W^2 - 1} [1 + \exp\{\beta(W - 1) - \eta\}]^{-1} \times dW / (\pi^2 \lambda^3). \quad (4)$$

Here  $\lambda = \hbar / m_e c$ .  $Q_c$  is given by

$$Q_c = Q_m - [B_n(Z) - B_n(Z - 1)], \quad (5)$$

where

$$Q_m = Q_n - \left( \sum_{j_D=0}^{Z_D-1} \Delta_j - \sum_{j_P=0}^{Z_P-1} \Delta_j \right). \quad (6)$$

$Q_n$  is the neutral atom  $Q$  value of  $\beta^-$  transition and  $Q_m$  is the IPD modified  $Q$  value.  $\Delta_j$  is the ionization potential depression [4]. The term  $[B_n(Z) - B_n(Z - 1)]$  denotes the difference of binding energies for bound electrons of the daughter and the parent atom. The experimental values for all the atomic data (binding energies and ionization potential) are taken from Ref. [20].

Certain combinations of electron radial wave functions evaluated at nuclear radius  $R$  (in the unit of  $\hbar / m_e c$ ) were first introduced by Konopinski and Uhlenbeck [22] as  $L_k$ 's. Behrens and Jänecke [23] precisely calculated  $L_0$  for nuclei close to the valley of stability. To cover all isotopes between the proton and neutron drip lines for  $Z \leq 60$ , Wilkinson [24] provided a momentum dependent fitted expression of  $L_0$ ,

$$L_0 = 1 + \frac{13}{60} (\alpha Z)^2 - \frac{\alpha Z W R (41 - 26\gamma)}{15(2\gamma - 1)} - \frac{\alpha Z R \gamma (17 - 2\gamma)}{30W(2\gamma - 1)} + a_{-1} \frac{R}{W} + \sum_{n=0}^5 a_n (WR)^n + 0.41(R - 0.0164)(\alpha Z)^{4.5}, \quad (7)$$

with  $\gamma = \sqrt{1 - (\alpha Z)^2}$ . Here,  $\alpha$  is the fine structure constant. The parameter  $a_n$  (for  $n = -1$  to 5) is defined as

$$a_n = \sum_{x=1}^6 b_{x,n} (\alpha z)^x. \quad (8)$$

Details of  $b_{x,n}$  are discussed in Refs. [24,25].

Quantities presented in this paper are also worked out with momentum independent  $L_0$  [22]:

$$L_0 = \frac{1 + \sqrt{1 - \alpha^2 Z^2}}{2}. \quad (9)$$

We found that decay rates with this  $L_0$  are within 1–2 % of the results presented in this paper. The decay rates and related quantities corresponding to momentum independent  $L_0$  are presented in the Supplemental Material of this paper [26].

In Eq. (2),  $W$  is the total energy of the  $\beta^-$  particle for a  $Z - 1 \rightarrow Z$  transition. Here the mass difference between initial (parent) and final (daughter) states of neutral atoms is expressed as the decay  $Q$  value ( $Q_n$  in keV). The term

$F_0(Z, W)$  is the Fermi function for allowed transition given by [22]

$$F_0(Z, W) = \frac{4}{|\Gamma(1 + 2\gamma)|^2} \times (2R\sqrt{W^2 - 1})^{2(\gamma-1)} \exp\left[\frac{\pi\alpha ZW}{\sqrt{W^2 - 1}}\right] \times \left| \Gamma\left(\gamma + i\frac{\alpha ZW}{\sqrt{W^2 - 1}}\right) \right|^2. \quad (10)$$

Furthermore, for the bound state  $\beta^-$  decay of the bare atom  $f_a^*$  takes the form [4]

$$f_a^*(\text{Bound}) = \sum_x \sigma_x (\pi/2) g_x^2 b_x^2 \quad (\text{for } x = ns_{1/2}, np_{1/2}). \quad (11)$$

Here  $g_x$  is the large component of the electron radial wave function evaluated at the nuclear radius  $R$  of the daughter for the orbit  $x$ . The  $g_x$  is obtained by solving Dirac radial wave equations [27]. Here  $x$  is taken as  $1s_{1/2}$ ,  $2s_{1/2}$ ,  $3s_{1/2}$ , and  $4s_{1/2}$ . The effect of  $np_{1/2}$  wave functions is negligible. In this case,  $\sigma_x$  is the relative vacancy of the orbit, which in the case of bare atoms is 1, and  $b_x = Q_b / m_e c^2$ , where

$$Q_b = Q_m - [B_n(Z) - B_n(Z - 1)] + B_{\text{shell}}(Z). \quad (12)$$

For example, in the case of a bare atom, if the emitted  $\beta^-$  particle gets absorbed in the atomic  $K$  shell, then the last term of Eq. (12) will be the ionization potential for the  $K$  electron denoted by  $B_K(Z)$ , and a positive value for it has been used. In Ref. [15], Eq. (15) is the same as Eq. (12) of this paper. In Ref. [15] we used a negative value for the ionization potential. The effect of IPD on  $f_a^*$  is discussed in Sec. III B 2.

## B. Population of excited nuclear energy levels in the thermodynamic equilibrium

In a stellar environment due to high temperature, there is a definite probability of an equilibrium population of excited nuclear levels given by the Boltzmann distribution. These excited levels may also decay via  $\beta^-$  emission. Thus to incorporate these decays, we take the equilibrium population derived from

$$\frac{n_{ik+1}}{n_{ik}} = \frac{b_{ik+1}}{b_{ik}} \exp(-\Delta E_{ik} / k_B T), \quad (13)$$

where the fractional population of the element  $i$  in its  $k$ th nuclear state is expressed as  $n_{ik}$ .  $b_{ik}$  is the multiplicity of the  $k$ th state and  $\Delta E_{ik}$  is the energy difference between  $k$ th and  $(k + 1)$ th nuclear levels. Change in the ground state and excited state population in thermal equilibrium in the parent due to the reverse  $\beta$  decay of the daughter is not possible for any of the nuclei considered.

The total stellar  $\beta^-$  decay rate ( $\lambda_{\text{bare}(s)}$ ) of a bare atom is given by

$$\lambda_{\text{bare}(s)} = \sum_k \left( n_{ik} \sum_m \lambda_{km} \right), \quad (14)$$

where  $\lambda_{km} = \lambda_b + \lambda_c$  is the  $\beta^-$  decay rate of bare atoms from the  $k$ th level of the parent nucleus to the  $m$ th level of the daughter nucleus.  $\lambda_b$  and  $\lambda_c$  are the rates for the decays to the bound and continuum states, respectively.

### C. Calculation of $\log ft$

In the case of  $\beta^-$  decay the comparative half-life  $ft$  corresponding to each transition can be calculated using [28]

$$ft = \frac{6177}{((g_A/g_V)q)^2 B(GT) + B(F)} \text{ s.} \quad (15)$$

The factor  $B(GT)$  is the reduced Gamow-Teller (GT) strength, from which one can define a matrix element  $M(GT)$  as [28]

$$M(GT) = \sqrt{(2J_i + 1)B(GT)}. \quad (16)$$

$B(F)$  is the reduced Fermi strength.  $J_i$  is the total angular momentum of the parent state.  $g_A$  and  $g_V$  are the weak interaction vector and axial-vector coupling constants for the decay of a neutron to a proton, respectively. The ‘‘free nucleon’’ (i.e., for the decay of a neutron to a proton) value of  $|g_A/g_V|$  is [29]

$$|g_A/g_V| = 1.2606 \pm 0.0075. \quad (17)$$

The concept of quenching of GT strength arose out of the fact that the sum rule observed in experiment is in general less than that predicted by shell-model calculations. The ratio of observed strength and predicted strength is taken as the  $q$  factor. Quenching factor  $q$  is used as the normalization of the GT operator which is understood as general inadequacies inherent in the truncated shell-model calculation.

Thus comparison between experimental and theoretical  $M(GT)$  leads to the Gamow-Teller strength quenching factor  $q$ . This is further discussed in Appendix B.

## III. RESULTS AND DISCUSSION

### A. Shell-model calculations of $ft$ values

In the terrestrial scenario, the  $\log ft$  values of  $\beta^-$  transitions from parent ground state and/or isomeric state to the daughter states are available for most of the cases considered in the mass region  $A = 59-81$ . However, in the stellar  $s$ -process situation, as discussed before, thermally populated excited states may also undergo  $\beta^-$  decay to various daughter levels. Evidently, no experimental data corresponding to these  $\beta^-$  decays from the excited states are available. So, one has to rely on theoretical predictions. Therefore, we have performed shell-model calculations in the  $(1f_{7/2}2p_{3/2}1f_{5/2}2p_{1/2})$  and  $(2p_{3/2}1f_{5/2}2p_{1/2}1g_{9/2})$  valance spaces with  $^{40}\text{Ca}$  and  $^{56}\text{Ni}$  cores, respectively. These two model spaces cover all nuclei in the considered range. The shell-model calculations have been carried out with the OXBASH [30] and the NUSHELLX [31] codes. The energy eigenfunctions obtained for the parent and the daughter nuclei are used to calculate the reduced Fermi ( $B(F)$ ) and the Gamow-Teller ( $B(GT)$ ) strengths. These matrix elements are then used to calculate the  $ft$  values for each transition [Eq. (15)], allowed by the  $Q$  value of the decay. In these model spaces, shell-model calculations are difficult to

perform in some cases because of prohibitively large dimensionalities. For those cases we performed moderately large basis shell model (LBSM) calculations with reasonable and judicious truncation (see Appendix A).

In this work our primary aim is to reproduce experimental  $\log ft$  values theoretically within the shell-model framework. Thus for each nucleus these values are calculated with various available interaction Hamiltonians. Later, for each nucleus, an appropriate interaction was chosen which reproduced the data most successfully.

We have checked that the use of average quenching factors for fp and fpg spaces have limited predictability [32] of  $\log ft$  values for GT transitions in various nuclei. One may also expect a dependence of the quenching factor on  $A$ ,  $(N-Z)$ , and the shell closure [28]. So, we found it advantageous to determine the quenching factor for each nucleus while calculating  $\log ft$  values.

The method to obtain the quenching factor  $q$  of the GT strength is as follows:

- (i) In the case of a single  $\beta^-$  transition from the ground state and/or isomeric state the quenching factor is chosen as 1, and the same  $q$  is used for  $\beta^-$  transition from excited states of that parent nucleus, if any.
- (ii) In the case of multiple  $\beta^-$  transitions from the ground state and/or isomeric state of the parent, the quenching factor was obtained from the slope of the fitting of  $M(GT)_{\text{expt}}$  with  $M(GT)_{\text{theor}}$ . The same  $q$  is used for  $\beta^-$  transitions from the excited levels of the same nucleus. See Appendix B for details (exception:  $^{61}\text{Co}$ ,  $^{78}\text{Ge}$ ).

For the cases of  $^{61}\text{Co}$  and  $^{78}\text{Ge}$ , we have taken  $q = 1$ , since for each of them, experimental  $\log ft$  values for only two transitions are available. In the case of  $^{61}\text{Co}$ , the  $7/2^-_1$  ground state can decay to five levels of  $^{61}\text{Ni}$ . However, experimental  $\log ft$  values for only two transitions are available. Similarly, for the case of  $^{78}\text{Ge}$ , the  $0^+_1$  ground state can decay to three  $1^+$  states of  $^{78}\text{As}$ . But experimental  $\log ft$  values for only the first and second  $1^+$  states are available. Thus the experimental information is incomplete to obtain the  $q$  values.

We present, in Table I, only the calculated  $\log ft$  values which closely agree with the experimental ones. The  $\log ft$  values of transitions in a nucleus are calculated with a single Hamiltonian appropriate for that nucleus as selected from the comparisons as discussed above. In this table, we show the results for energy eigenvalues of parent and daughter also, which are relevant here, along with the derived quenching factor  $q$ .

In Fig. 1, we show a summary of the results based on Table I, in the form of a statistics of the deviation of the calculated  $\log ft$  value from the corresponding experimental one. The figure shows that the predicted  $\log ft$  values agree with the experimental results in most cases. Larger deviations are found to be associated with the very weak  $\beta^-$  branchings. For example, for the  $^{72}\text{Zn} \rightarrow ^{72}\text{Ga}$   $\beta^-$  decay, with two transitions  $0^+_1 \rightarrow (0^+_1)$  and  $0^+_1 \rightarrow (1, 2)$ ,  $\log ft$  values [19] are given as  $>8.6$  and  $7.2$ , respectively. However, it is mentioned in Ref. [19] that the existence of these branches [0.01% and



TABLE I. Comparison of experimental [19] and calculated  $\log ft$ . Here,  $E_p$  and  $E_d$  correspond to the parent and daughter level energies in keV, respectively. Errors in the experimental energy levels [19] are mentioned in the brackets.  $J_p^\pi$  and  $J_d^\pi$  are the spin parities of the parent and daughter levels, respectively.  $q$  is the quenching factor. The name of the interaction Hamiltonian used for each nucleus is given in column 7. In the cases where the spin parity ( $J^\pi$ ) of a level is unconfirmed in Ref. [19], we have decided  $J^\pi$  from shell model calculation. Here, ‘‘Expt.’’ stands for experimental values [19] and ‘‘Theor.’’ stands for present shell-model calculation.

Decay	Transition details					Shell-model results								
	Parent level		Daughter level		Expt. $\log ft$	Interaction	$q$	$E_p$	$E_d$	Theor. $\log ft$				
	$J_p^\pi$	$E_p$	$J_d^\pi$	$E_d$										
$^{59}\text{Fe} \rightarrow ^{59}\text{Co}$	$3/2_1^-$	0.0	$3/2_1^-$	1099.256(3)	6.696(13)	fpd6	0.82	0	1139	6.718				
			$3/2_2^-$	1291.605(5)	5.979(11)				2398	5.902				
			$1/2_1^-$	1434.256(5)	6.482(18)				2496	7.060				
			$5/2_1^-$	1481.72(12)	7.10(4)				1337	7.759				
	$1/2_1^-$	287.023(19)	$3/2_1^-$	1099.256(3)						246	1139	7.011		
			$3/2_2^-$	1291.605(5)						2398	6.508			
			$1/2_1^-$	1434.256(5)						2496	5.770			
	$5/2_1^-$	472.87(9)	$7/2_1^-$	0.0						128	0	5.318		
			$3/2_1^-$	1099.256(3)							1139	6.772		
			$3/2_2^-$	1291.605(5)							2398	7.611		
			$5/2_1^-$	1481.72(12)							1337	8.250		
			$7/2_2^-$	1744.69(20)							1494	6.220		
$^{60}\text{Co} \rightarrow ^{60}\text{Ni}$	$5_1^+$	0.0	$4_1^+$	2505.753(4)	7.512(2)	fpd6pn	0.58	0	2242	7.313				
			$2_1^+$	1332.514(4)	7.2				173	1326	7.349			
	$2_1^+$	58.59(1)	$2_2^+$	2158.632(18)	7.4						2095	7.423		
			$4_1^+$	2505.753(4)						239	2242	6.445		
	$4_1^+$	277.20(2)	$3_1^+$	2626.06(5)							1908	7.112		
			$3_1^+$	288.40(2)	$2_1^+$			1332.514(4)				415	1326	6.892
	$3_1^+$	288.40(2)	$2_2^+$	2158.632(18)								2095	7.242	
			$4_1^+$	2505.753(4)								2242	6.897	
			$3_1^+$	2626.06(5)								2202	8.331	
			$5_2^+$	435.71(4)	$4_1^+$			2505.753(4)				461	2242	6.996
			$4_2^+$	3119.87(7)								2595	7.289	
	$^{61}\text{Co} \rightarrow ^{61}\text{Ni}$	$7/2_1^-$	0.0	$5/2_1^-$	67.414(7)			5.240(3)	fpd6n	1.00	0	221	5.292	
$5/2_2^-$				908.613(11)				783				5.981		
$(7/2)_1^-$				917.5(7)	4.78(4)			1134				5.788		
$7/2_2^-$				1015.24(8)				1546				5.949		
$5/2_3^-$				1132.347(18)				1118				5.226		
$^{63}\text{Ni} \rightarrow ^{63}\text{Cu}$	$1/2_1^-$	0.0	$3/2_1^-$	0.0	6.7	fpd6npn	1.00	7	0	6.318				
			$5/2_1^-$	87.15(11)	$3/2_1^-$				0.0			0	0	5.747
			$3/2_1^-$	155.55(15)	$3/2_1^-$				0.0			238	0	5.323
$^{65}\text{Ni} \rightarrow ^{65}\text{Cu}$	$5/2_1^-$	0.0	$3/2_1^-$	0.0	6.576(2)	jun45	0.63	8	0	6.592				
			$5/2_1^-$	1115.556(4)	6.064(6)						1570	6.406		
			$7/2_1^-$	1481.83(3)	4.901(4)						1516	4.933		
			$5/2_2^-$	1623.43(5)	6.03(1)						2074	5.609		
			$3/2_2^-$	1725.00(5)	5.90(1)						2155	6.370		
			$(7/2)_2^-$	2094.34(14)							2164	4.385		
			$(5/2)_3^-$	2107.44(13)							2425	7.556		
	$1/2_1^-$	63.37(5)	$3/2_1^-$	0.0						0	0	4.567		
			$1/2_1^-$	770.64(9)							931	6.155		
			$3/2_2^-$	1725.00(5)							2155	6.249		
	$3/2_1^-$	310.08(22)	$3/2_1^-$	0.0						599	0	5.561		
			$1/2_1^-$	770.64(9)							931	7.166		
$5/2_1^-$			1115.556(4)					1570	6.078					
$5/2_2^-$			1623.43(5)					2074	6.446					

TABLE I. (Continued.)

Decay	Transition details				Expt. log $ft$	Shell-model results											
	Parent level		Daughter level			Interaction	$q$	$E_p$	$E_d$	Theor. log $ft$							
	$J_p^\pi$	$E_p$	$J_d^\pi$	$E_d$													
$^{66}\text{Ni} \rightarrow ^{66}\text{Cu}$	$0_1^+$	0.0	$3/2_2^-$	1725.00(5)	4.3	fpd6n	1.0	0	2155	8.367							
			$(5/2)_3^-$	2107.44(13)					2425	5.637							
			$(1/2)_2^-$	2212.84(15)					2259	6.145							
			$3/2_3^-$	2329.05(15)					2345	6.768							
			$1_1^+$	0.0					0	0	4.307						
			$^{64}\text{Cu} \rightarrow ^{64}\text{Zn}$	$1_1^+$					0.0	$0_1^+$	0.0	5.302(5)	jun45	1.0	0	0	5.368
										$2_1^+$	1039.2279(21)	5.43	1059	5.203			
			$^{66}\text{Cu} \rightarrow ^{66}\text{Zn}$	$1_1^+$					0.0	$0_1^+$	0.0	5.33	jun45	0.51	67	0	5.575
										$2_1^+$	1039.2279(21)	5.43				1059	5.203
										$2_2^+$	1872.7653(24)	5.82(1)				2015	6.173
$0_2^+$	2372.353(4)	6.01(4)			2550	6.562											
$2_1^+$	185.953(15)	$2_1^+$			1039.2279(21)	0	1059	5.501									
		$2_2^+$			1872.7653(24)	2015	7.771										
		$2_3^+$			2780.157(7)	2695	6.440										
$3_1^+$	275.030(17)	$2_1^+$			1039.2279(21)	13	1059	7.925									
		$2_2^+$			1872.7653(24)	2015	8.216										
		$4_1^+$			2451.01(5)	2451	5.244										
		$4_2^+$	2765.56(7)	2633	5.920												
		$2_3^+$	2780.157(7)	2695	6.294												
	$(1_2^+)$	385.782(10)	$0_1^+$	0.0					94	0	6.085						
			$2_1^+$	1039.2279(21)					1059	5.290							
			$2_2^+$	1872.7653(24)					2015	5.955							
			$0_2^+$	2372.353(4)					2550	6.949							
			$2_3^+$	2780.157(7)					2695	6.597							
			$2_4^+$	2938.074(3)					2957	5.643							
			$2_2^+$	465.165(10)					$2_1^+$	1039.2279(21)	61	1059	5.911				
									$2_2^+$	1872.7653(24)	2015	6.011					
									$2_3^+$	2780.157(7)	2695	6.669					
									$2_4^+$	2938.074(3)	2957	6.228					
$^{67}\text{Cu} \rightarrow ^{67}\text{Zn}$	$3/2_1^-$	0.0	$5/2_1^-$	0.0	$\approx 6.3$	fpd6n	0.65	0	183	5.976							
			$1/2_1^-$	93.312(5)	$\approx 6.0$				0	5.976							
			$3/2_1^-$	184.579(6)	$\approx 5.2$				153	5.430							
			$3/2_2^-$	393.531(7)	$\approx 5.8$				483	5.535							
$^{69}\text{Zn} \rightarrow ^{69}\text{Ga}$	$1/2_1^-$	0.0	$3/2_1^-$	0.0	4.48(1)	fpd6n	0.93	0	0	4.482							
			$1/2_1^-$	318.706(21)	8.72(8)				53	7.654							
			$3/2_2^-$	871.147(22)	5.45(19)				773	5.434							
$^{72}\text{Zn} \rightarrow ^{72}\text{Ga}$	$0_1^+$	0.0	$(0_1^+)$	119.66(5)	$> 8.6$	jun45	0.73	0	253	7.321							
			$1_1^+, 2$	128.79(6)	7.2(3)				367	4.837							
			$1_2^+$	161.53(5)	4.468(12)				457	4.673							
			$1_3^+$	208.45(5)	4.972(17)				641	4.672							
$^{70}\text{Ga} \rightarrow ^{70}\text{Ge}$	$1_1^+$	0.0	$0_1^+$	0.0	5.0925(18)	gx1	0.52	0	0	5.113							
			$2_1^+$	1039.506(9)	5.895(25)				1281	5.046							
			$0_2^+$	1215.621(15)	5.431(15)				3190	5.391							
$^{75}\text{Ge} \rightarrow ^{75}\text{As}$	$1/2_1^-$	0.0	$3/2_1^-$	0.0	5.175(7)	jun45	0.25	0	0	5.180							
			$1/2_1^-$	198.6063(8)	6.87(5)				281	7.160							
			$3/2_2^-$	264.6581(6)	5.63(5)				788	5.644							
			$1/2_2^-$	468.74(17)	6.94(5)				1757	7.080							
			$1/2_3^-$	585(7)					2014	5.476							
			$1/2^-, 3/2_3^-$	617.68(4)	6.42(6)				1355	6.242							
			$(3/2_4^-, 5/2^-)$	865.4(5)					1769	7.336							
			$3/2_5^-$	1063.3(5)					2068	8.807							
			$3/2_6^-$	1074.5(7)					2292	7.021							

TABLE I. (Continued.)

Decay	Transition details				Shell-model results					
	Parent level		Daughter level		Expt. log $ft$	Interaction	$q$	$E_p$	$E_d$	Theor. log $ft$
	$J_p^\pi$	$E_p$	$J_d^\pi$	$E_d$						
			$1/2_4^-, 3/2^-$ ( $1/2_3^- to 7/2^-$ )	1127(6) 1172.0(6)				2624 2870	7.020 5.975	
	$7/2_1^+$	139.69(3)	$9/2_1^+$ $5/2_1^+$ ( $5/2_2^+$ ) ( $5/2_3^+, 7/2^-$ ) $9/2_2^+$ $5/2_4^+$	303.9243(8) 400.6583(6) 1080.8(8) 1100.2(6) 1261(5) 1302.3(7)	6.21(13)			13 2338 2551 2997 3085 2572 3116	7.414 7.090 5.964 6.836 6.556 6.152	
	$5/2_1^+$	192.19(6)	$5/2_1^+$ ( $5/2_2^+$ ) ( $5/2_3^+, 7/2^-$ ) $5/2_4^+$	400.6583(6) 1080.8(8) 1100.2(6) 1302.3(7)				9 2551 2997 3085 3116	6.584 5.809 6.030 5.852	
	$9/2_1^+$	199.89(11)	$9/2_1^+$ $9/2_2^+$	303.9243(8) 1261(5)				183 2338 2572	6.901 6.979	
	$3/2_1^-$	253.15(6)	$3/2_1^-$ $1/2_1^-$ $3/2_2^-$ $5/2_1^-$ $1/2_2^-$ $5/2_2^-$ $1/2_3^-$ $1/2^-, 3/2_3^-$ ( $3/2_4^-, 5/2^-$ ) $3/2_5^-$ $3/2_6^-$ $1/2_4^-, 3/2^-$ ( $1/2_5^- to 7/2^-$ ) $3/2_7^-$ $3/2_8^-$ ( $3/2^-$ ) <sub>9</sub> ( $5/2^-$ ) <sub>3</sub>	0.0 198.6063(8) 264.6581(6) 279.5428(8) 468.74(17) 572.41(3) 585(7) 617.68(4) 865.4(5) 1063.3(5) 1074.5(7) 1127(6) 1172.0(6) 1203.5(6) 1349.4(6) 1370.8(7) 1420.2(5)			434	0 281 788 600 1757 841 2014 1355 1769 2068 2292 2652 2624 2770 2984 3052 1047	5.725 5.796 6.262 7.960 7.883 6.913 7.289 6.583 6.504 6.084 7.186 6.757 6.757 6.534 6.799 6.080 6.055	
	$5/2_1^-$	316.81(7)	$3/2_1^-$ $3/2_2^-$ $5/2_1^-$ $5/2_2^-$ $1/2^-, 3/2_3^-$ $7/2_1^-$ ( $3/2_4^-, 5/2^-$ ) $7/2_2^-$ $3/2_5^-$ $3/2_6^-$ ( $7/2^-$ ) <sub>3</sub> ( $5/2^+, 7/2_4^-$ ) $3/2_7^-$ $7/2_5^-$ $3/2_8^-$ ( $3/2^-$ ) <sub>9</sub> ( $5/2^-$ ) <sub>3</sub> $3/2_{10}^-$	0.0 264.6581(6) 279.5428(8) 572.41(3) 617.68(4) 821.62(15) 865.4(5) 1043.4(6) 1063.3(5) 1074.5(7) 1096.3(7) 1100.2(6) 1203.5(6) 1309.5(4) 1349.4(6) 1370.8(7) 1420.2(5) 1430.5(6)			48	0 788 599 841 1355 576 1769 1467 2068 2292 1743 1992 2652 2493 2770 2984 1046 3052	6.529 6.556 6.030 6.312 7.048 5.264 7.401 6.075 7.248 9.850 7.251 6.745 7.349 6.283 8.363 7.270 5.915 7.015	
	$5/2_2^-$	457.07(7)	$3/2_1^-$ $3/2_2^-$ $5/2_1^-$	0.0 264.6581(6) 279.5428(8)				374 788 599	7.128 8.497 7.989	

TABLE I. (Continued.)

Decay	Transition details					Shell-model results												
	Parent level		Daughter level		Expt. log <i>ft</i>	Interaction	<i>q</i>	<i>E<sub>p</sub></i>	<i>E<sub>d</sub></i>	Theor. log <i>ft</i>								
	<i>J<sub>p</sub><sup>π</sup></i>	<i>E<sub>p</sub></i>	<i>J<sub>d</sub><sup>π</sup></i>	<i>E<sub>d</sub></i>														
<sup>78</sup> Ge → <sup>78</sup> As	0 <sub>1</sub> <sup>+</sup>	0.0	5/2 <sub>2</sub> <sup>-</sup>	572.41(3)	4.264(25)	jun45	1.00	0	841	6.645								
			1/2 <sup>-</sup> , 3/2 <sub>3</sub> <sup>-</sup>	617.68(4)					1355	8.312								
			7/2 <sub>1</sub> <sup>-</sup>	821.62(15)					576	6.053								
			(3/2 <sub>4</sub> <sup>-</sup> , 5/2 <sup>-</sup> )	865.4(5)					1769	9.618								
			7/2 <sub>2</sub> <sup>-</sup>	1043.4(6)					1467	7.110								
			3/2 <sub>5</sub> <sup>-</sup>	1063.3(5)					2068	7.444								
			3/2 <sub>6</sub> <sup>-</sup>	1074.5(7)					2292	8.669								
			(7/2 <sup>-</sup> ) <sub>3</sub>	1096.3(7)					1743	6.731								
			(5/2 <sup>+</sup> , 7/2 <sub>4</sub> <sup>-</sup> )	1100.2(6)					1992	6.836								
			3/2 <sub>7</sub> <sup>-</sup>	1203.5(6)					2652	7.522								
			7/2 <sub>5</sub> <sup>-</sup>	1309.5(4)					2493	8.629								
			3/2 <sub>8</sub> <sup>-</sup>	1349.4(6)					2770	8.833								
			(3/2 <sup>-</sup> ) <sub>9</sub>	1370.8(7)					2984	8.667								
			(5/2 <sup>-</sup> ) <sub>3</sub>	1420.2(5)					1046	6.777								
			3/2 <sub>10</sub> <sup>-</sup>	1430.5(6)					3052	7.934								
1/2 <sup>-</sup> , 3/2 <sub>11</sub> <sup>-</sup>	1606.3(5)	3097	7.789															
<sup>81</sup> Se → <sup>81</sup> Br	1/2 <sub>1</sub> <sup>-</sup>	0.0	1 <sub>1</sub> <sup>+</sup>	277.3(3)	5.010(4)	jun45	0.62	29	0	0	5.047							
			1 <sub>2</sub> <sup>+</sup>	293.9(5)					518	5.046								
			1 <sub>3</sub> <sup>+</sup>	536(4)					593	3.875								
<sup>81</sup> Se → <sup>81</sup> Br	7/2 <sub>1</sub> <sup>+</sup>	103.00(6)	3/2 <sub>1</sub> <sup>-</sup>	0.0	8.25(22)	jun45	0.62	29	0	0	5.047							
			1/2 <sub>1</sub> <sup>-</sup> , 3/2 <sup>-</sup>	538.20(8)					351	7.957								
			3/2 <sub>2</sub> <sup>-</sup>	566.04(5)					671	7.297								
			(3/2 <sup>-</sup> ) <sub>3</sub>	649.90(8)					793	6.901								
			3/2 <sub>4</sub> <sup>-</sup>	828.29(5)					1162	5.870								
			(1/2 <sub>2</sub> <sup>-</sup> )	1105.3(6)					908	6.625								
			(3/2 <sub>5</sub> <sup>-</sup> , 5/2, 7/2 <sup>-</sup> )	1266.8(6)					1865	6.998								
			(3/2 <sup>-</sup> ) <sub>6</sub>	1535.9(7)					1921	6.849								
			(3/2 <sup>-</sup> ) <sub>7</sub>	1543.2(5)					1991	6.391								
			9/2 <sub>1</sub> <sup>+</sup>	536.20(9)					0	2042	8.068							
			7/2 <sub>1</sub> <sup>+</sup>	1371.5(13)					2390	5.528								
			(9/2 <sup>+</sup> ) <sub>2</sub>	1541.6(13)					2643	5.050								
			<sup>81</sup> Se → <sup>81</sup> Br	9/2 <sub>1</sub> <sup>+</sup>					294.30(17)	9/2 <sub>1</sub> <sup>+</sup>	536.20(9)	8.25(22)	jun45	0.62	29	171	2042	7.074
										7/2 <sub>1</sub> <sup>+</sup>	1371.5(13)					2390	6.427	
										(11/2 <sup>+</sup> ) <sub>1</sub>	1522.3(8)					2454	6.900	
(9/2 <sup>+</sup> ) <sub>2</sub>	1541.6(13)	2643			5.113													
(7/2 <sup>+</sup> ) <sub>2</sub>	1788.9(13)	2481			5.804													
3/2 <sub>1</sub> <sup>-</sup>	467.74(8)	638			0	5.400												
<sup>81</sup> Se → <sup>81</sup> Br	3/2 <sub>1</sub> <sup>-</sup>	467.74(8)	3/2 <sub>1</sub> <sup>-</sup>	0.0	8.25(22)	jun45	0.62	29	638	0	5.400							
			5/2 <sub>1</sub> <sup>-</sup>	275.985(12)					541	6.257								
			1/2 <sub>1</sub> <sup>-</sup> , 3/2 <sup>-</sup>	538.20(8)					351	7.837								
			3/2 <sub>2</sub> <sup>-</sup>	566.04(5)					671	6.138								
			(3/2 <sub>3</sub> <sup>-</sup> )	649.90(8)					793	8.761								
			(5/2 <sup>-</sup> ) <sub>2</sub>	767.04(9)					538	5.530								
			3/2 <sub>4</sub> <sup>-</sup>	828.29(5)					1162	6.937								
			5/2 <sub>3</sub> <sup>(-)</sup>	1023.7(4)					845	6.439								
			(1/2 <sub>2</sub> <sup>-</sup> )	1105.3(6)					908	6.664								
			5/2 <sub>4</sub> <sup>-</sup> , 7/2 <sup>-</sup>	1189.9(21)					993	7.169								
			(3/2 <sub>5</sub> <sup>-</sup> , 5/2, 7/2 <sup>-</sup> )	1266.8(6)					1865	6.181								
			(5/2 <sub>5</sub> <sup>-</sup> )	1323.0(4)					1578	6.654								
			(3/2 <sub>6</sub> <sup>-</sup> , 1/2 <sup>-</sup> )	1512.9(10)					1921	5.938								
			(3/2 <sup>-</sup> ) <sub>7</sub>	1535.9(7)					1991	5.989								
			(3/2 <sup>-</sup> ) <sub>8</sub>	1543.2(5)					2267	5.749								
(5/2 <sup>-</sup> ) <sub>6</sub>	1798.9(10)	1902	6.388															



TABLE I. (Continued.)

Decay	Transition details				Expt. $\log ft$	Shell-model results			
	Parent level		Daughter level			Interaction	$q$	$E_p$	$E_d$
	$J_p^\pi$	$E_p$	$J_d^\pi$	$E_d$					
			$(3/2^-)_9$	1866.4(10)				2399	6.561
			$(3/2^-_{10}, 5/2^-, 7/2^-)$	1885.2(7)				2507	5.769
	$(5/2^-)_1$	491.06(9)	$3/2^-_1$	0.0			479	0	8.745
			$5/2^-_1$	275.985(12)				541	5.346
			$3/2^-_2$	566.04(5)				671	7.250
			$(3/2^-)_3$	649.90(8)				793	7.514
			$(5/2^-)_2$	767.04				538	6.188
			$3/2^-_4$	828.29(5)				1162	7.817
			$7/2^-_1$	836.78(9)				834	6.138
			$5/2^-_{(3)}$	1023.7(4)				845	7.221
			$5/2^-_4, 7/2^-$	1189.9(21)				993	6.752
			$(3/2^-_5, 5/2^-, 7/2^-)$	1266.8(6)				1865	8.336
			$(5/2^-)_5$	1323.0(4)				1578	6.263
			$(7/2^-)_2$	1481.7(6)				986	5.337
			$(3/2^-_6, 1/2^-)$	1512.9(10)				1921	6.905
			$(3/2^-)_7$	1535.9(7)				1991	7.989
			$(3/2^-)_8$	1543.2(5)				2267	6.980
			$(7/2^-)_3$	1681.2(8)				1549	6.134
			$(5/2^-)_6$	1798.9(10)				1902	7.432
			$(3/2^-)_9$	1866.4(10)				2399	7.836
			$(3/2^-_{10}, 5/2^-, 7/2^-)$	1885.2(7)				2507	7.206
			$7/2^-_{(4)}$	1995.9(8)				1742	4.583
			$1/2^-, 3/2^-_{11}$	2056.0(21)				2538	7.015

0.21(3)%, respectively] is questionable. These two  $\log ft$  values which deviate most from the theoretical ones are marked with an asterisk in Fig. 1. We have selected, out of the 48 transitions, 26 transitions that have  $\beta^-$  branching  $>5\%$  and have plotted the frequency distribution in the inner panel of Fig. 1. One can see that the calculated  $\log ft$  values are much closer to the experimental values. The deviation range reduced from  $(-1.2, +1.2)$  to  $(-0.6, +0.4)$ .

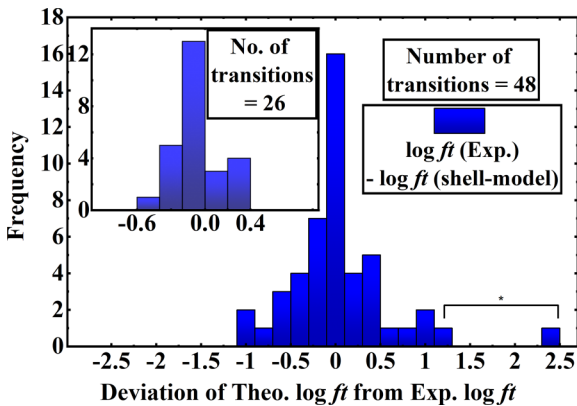


FIG. 1. The number of  $\log ft$  values as frequency vs difference between experimental and theoretical  $\log ft$  values of all the known transitions (48 in number) with a bin size of 0.3. See text for details.

In Fig. 2, the frequency distribution of the calculated  $\log ft$  of all 223 transitions is compared with that of the experimentally available allowed 225  $\log ft$  values, of the same mass region. The histograms clearly indicate that the calculated  $\log ft$  values are in good agreement with the experimental

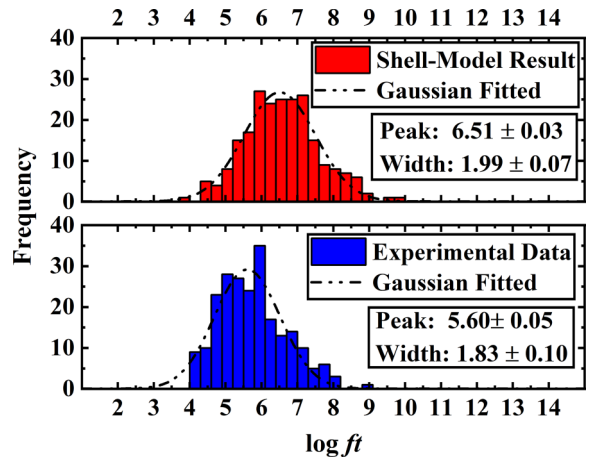


FIG. 2. The number of  $\log ft$  values as frequency is plotted as a function of  $\log ft$  values with a bin size of 0.3. Histograms are fitted with Gaussian curves in both of the plots, as shown. An overall similarity and agreement of the two distributions can be noted. See text for details.

TABLE II. A comparison of terrestrial half-lives ( $T_{1/2(t)}$ ).  $J_p^\pi$  and  $J_d^\pi$  are the spin parities of the parent and daughter levels, respectively. Experimental  $\beta^-$  branching ( $I_{m(\text{expt})}$ ) from a parent level given in Ref. [19] is normalized to 100%. Theoretical  $\beta^-$  branching ( $I_m$ ) calculations take into account only  $\beta^-$  decay from the parent levels.

Decay	Transition details [19]			Shell-model results	
	$J_p^\pi \rightarrow J_d^\pi$	Expt. $\beta^-$ $I_m(\%)$	Expt. $T_{1/2(t)}$	Theor. $\beta^-$ $I_m(\%)$	Theor. $T_{1/2(t)}$
$^{59}\text{Fe} \rightarrow ^{59}\text{Co}$	$3/2_1^- \rightarrow 3/2_1^-$	53.1	44.490 d	48.10	41.21 d
	$3/2_1^- \rightarrow 3/2_2^-$	45.3		51.55	
	$3/2_1^- \rightarrow 1/2_1^-$	1.31		0.33	
	$3/2_1^- \rightarrow 5/2_1^-$	0.078		0.02	
$^{60}\text{Co} \rightarrow ^{60}\text{Ni}$	$5_1^+ \rightarrow 4_1^+$	100.0	1925.28 d	100.00	1198.71 d
	$^{a,b} 2_1^+ \rightarrow 2_1^+$	96	2.91 d	95.68	5.41 d
	$^{a,b} 2_1^+ \rightarrow 2_2^+$	4		4.32	
$^{61}\text{Co} \rightarrow ^{61}\text{Ni}$	$7/2_1^- \rightarrow 5/2_1^-$	95.6	1.649 hr	98.86	1.87 hr
	$7/2_1^- \rightarrow 5/2_2^-$			0.35	
	$7/2_1^- \rightarrow 7/2_1^-$	4.4		0.50	
	$7/2_1^- \rightarrow 7/2_2^-$			0.14	
	$7/2_1^- \rightarrow 5/2_3^-$			0.15	
$^{63}\text{Ni} \rightarrow ^{63}\text{Cu}$	$1/2_1^- \rightarrow 3/2_1^-$	100.0	101.2 yr	100.00	44.69 yr
$^{65}\text{Ni} \rightarrow ^{65}\text{Cu}$	$5/2_1^- \rightarrow 3/2_1^-$	60.0	2.51 hr	63.08	2.67 hr
	$5/2_1^- \rightarrow 5/2_1^-$	10.18		5.07	
	$5/2_1^- \rightarrow 7/2_1^-$	28.4		29.07	
	$5/2_1^- \rightarrow 5/2_2^-$	0.89		2.58	
	$5/2_1^- \rightarrow 3/2_2^-$	0.555		0.21	
	$5/2_1^- \rightarrow 7/2_2^-$			0.01	
$5/2_1^- \rightarrow 5/2_3^-$		<0.01			
$^{66}\text{Ni} \rightarrow ^{66}\text{Cu}$	$0_1^+ \rightarrow 1_1^+$	100	54.6 hr	100	57.96 hr
$^{64}\text{Cu} \rightarrow ^{64}\text{Zn}$	$1_1^+ \rightarrow 0_1^+$	100	32.9886 hr	100	37.27 hr
$^{66}\text{Cu} \rightarrow ^{66}\text{Zn}$	$1_1^+ \rightarrow 0_1^+$	90.77	5.120 min	77.12	7.42 min
	$1_1^+ \rightarrow 2_1^+$	9.01		22.73	
	$1_1^+ \rightarrow 2_2^+$	0.220		0.14	
	$1_1^+ \rightarrow 0_2^+$	0.0037		0.00	
$^{67}\text{Cu} \rightarrow ^{67}\text{Zn}$	$3/2_1^- \rightarrow 5/2_1^-$	$\approx 20$	61.83 hr	40.64	68.61 hr
	$3/2_1^- \rightarrow 1/2_1^-$	$\approx 22$		21.50	
	$3/2_1^- \rightarrow 3/2_1^-$	$\approx 57$		35.87	
	$3/2_1^- \rightarrow 3/2_2^-$	$\approx 1.1$		1.99	
$^{69}\text{Zn} \rightarrow ^{69}\text{Ga}$	$1/2_1^- \rightarrow 3/2_1^-$	99.9986	56.4 min	99.99	53.77 min
	$1/2_1^- \rightarrow 1/2_1^-$	0.0012		0.01	
	$1/2_1^- \rightarrow 3/2_2^-$	0.00025		$\approx 0.00$	
$^{72}\text{Zn} \rightarrow ^{72}\text{Ga}$	$0_1^+ \rightarrow 0_1^+$	<0.01	46.5 hr		54.56 hr
	$0_1^+ \rightarrow 1_1^+$	0.21			
	$0_1^+ \rightarrow 1_2^+$	85.1		64.42	
	$0_1^+ \rightarrow 1_3^+$	14.7		35.58	
$^{70}\text{Ga} \rightarrow ^{70}\text{Ge}$	$1_1^+ \rightarrow 0_1^+$	98.91	21.23 min	97.01	21.09 min
	$1_1^+ \rightarrow 2_1^+$	0.36		2.63	
	$1_1^+ \rightarrow 0_2^+$	0.32		0.36	
$^{75}\text{Ge} \rightarrow ^{75}\text{As}$	$1/2_1^- \rightarrow 3/2_1^-$	87.1	82.78 min	84.52	78.94 min
	$1/2_1^- \rightarrow 1/2_1^-$	0.86		0.44	
	$1/2_1^- \rightarrow 3/2_2^-$	11.5		11.04	
	$1/2_1^- \rightarrow 1/2_2^-$	0.225		0.16	
	$1/2_1^- \rightarrow 1/2_3^-$			3.36	
	$1/2_1^- \rightarrow 3/2_3^-$	0.32		0.29	
	$1/2_1^- \rightarrow 3/2_4^-$			0.01	
	$1/2_1^- \rightarrow 3/2_5^-$			<0.01	
	$1/2_1^- \rightarrow 3/2_6^-$			<0.01	

TABLE II. (Continued.)

Decay	Transition details [19]			Shell-model results	
	$J_p^\pi \rightarrow J_d^\pi$	Expt. $\beta^-$ $I_m(\%)$	Expt. $T_{1/2(t)}$	Theor. $\beta^-$ $I_m(\%)$	Theor. $T_{1/2(t)}$
$^{78}\text{Ge} \rightarrow ^{78}\text{As}$	$1/2_1^- \rightarrow 1/2_4^-$			<0.01	
	$1/2_1^- \rightarrow 1/2_5^-$			<0.01	
	<sup>a,b</sup> $7/2_1^+ \rightarrow 5/2_1^+$	100	44.17 hr	100.00	326.17 hr
	$0_1^+ \rightarrow 1_1^+$	96	88 min	40.64	86.59 min
	$0_1^+ \rightarrow 1_2^+$	4		14.81	
$^{81}\text{Se} \rightarrow ^{81}\text{Br}$	$0_1^+ \rightarrow 1_3^+$			44.54	
	$1/2_1^- \rightarrow 3/2_1^-$	98.73	18.45 min	98.78	19.39 min
	$1/2_1^- \rightarrow 1/2_1^-$	0.034		0.02	
	$1/2_1^- \rightarrow 3/2_2^-$	0.79		0.10	
	$1/2_1^- \rightarrow 3/2_3^-$	0.0196		0.18	
	$1/2_1^- \rightarrow 3/2_4^-$	0.40		0.89	
	$1/2_1^- \rightarrow 1/2_2^-$			0.03	
	$1/2_1^- \rightarrow 3/2_5^-$			$\approx 0.01$	
	$1/2_1^- \rightarrow 3/2_6^-$			<0.01	
	$1/2_1^- \rightarrow 3/2_7^-$			<0.01	
	<sup>a,b</sup> $7/2_1^+ \rightarrow 9/2_1^+$	100	78.00 d	100	71.43 d

<sup>a</sup>Isomer.<sup>b</sup>Total  $\beta^-$  branching normalized to 100%. For example, the  $7/2_1^+$  isomer in  $^{75}\text{Ge}$  has only 0.03%  $\beta^-$  decay. We have taken this 0.03% as 100%.

values. The statistical properties, the peaks, centroids, and widths, calculated from the two histograms or from the Gaussian fits shown in the figure are similar. The upper panel of Fig. 2 includes transitions from the parent excited levels also, whereas, in the lower panel, transitions from the ground and isomeric levels of the nuclei are plotted. Close similarity and statistical behavior indicate the reliability of the calculated  $\log ft$  values for the  $\beta^-$  decay from excited nuclear levels.

In Table II we compare the terrestrial half-life obtained from theoretical  $\log ft$  values with the experimentally measured half-lives, for the set of nuclei. The good agreement between these once again indicates the acceptability of the calculated  $\log ft$  values.

We have noted that in some cases energy eigenvalues predicted by the shell-model calculations are not in agreement with the experimental level energies. However, the eigenfunctions of parent and daughter reproduce  $\log ft$  values which are reliable, as is evident from the agreement of the predicted half-lives with the experimental ones.

It is to be noted that for the phase space calculations, we used experimental [19]  $Q$  values and level energies.

One finds from Table II that the agreement of the calculated half-lives with the experimental values are good for most of the cases. However, for  $^{60}\text{Co}$  to  $^{60}\text{Ni}$  decay we obtained the terrestrial half-life  $T_{1/2(t)} = 3.285$  years instead of 5.275 years [19]. In the case of  $\beta^-$  decay from the isomeric  $2_1^+$  state of the same parent nucleus to the daughter states, the calculated  $T_{1/2(t)}$  is 5.41 days, whereas the experimental value is 2.91 days [19]. As shown in Ref. [19] these measurements are quite old. Moreover, the  $\beta^-$  decay from the isomeric state constitutes only 0.25% (0.1% in a measurement of the year 2010 [33]) [19] and is also a measurement of 1963 [34]. Because of these uncertainties in the measured values, it is difficult to

comment on the results for these transitions. Similar is the case for the decay from the isomeric level of  $^{75}\text{Ge}$ , which has  $\beta^-$  branching 0.03% only (measured in 1976 [35]); the disagreement of the calculated and measured  $T_{1/2(t)}$  is quite large. For  $^{63}\text{Ni}$  to  $^{63}\text{Cu}$  decay, we obtained  $T_{1/2(t)} = 44.69$  years, if the GT quenching factor  $q$  is taken as 1. If the globally accepted quenching factor  $q = 0.77$  was taken then the  $T_{1/2(t)}$  would have been about 75 years. It is well known that there is a difficulty in the measurement of long half-life as was the case of  $^{44}\text{Ti}$ . Our calculated half-life for  $^{63}\text{Ni}$  is not close to the measured [19]  $T_{1/2(t)} = 101.2(15)$  years. So, it is difficult to comment on this disagreement. We have also noted that there are slight disagreements of  $T_{1/2(t)}$  for the cases of  $\beta^-$  decay from  $^{67}\text{Cu}$  and  $^{72}\text{Zn}$ . In both of the cases, the measurements are old (1953 [36] and 1968 [37], respectively), and the measured branchings are quite uncertain.

## B. $\beta^-$ decay in stellar environment

As mentioned before, our calculation of the  $\beta^-$  decay rate is based on the  $s$ -process environment having temperature and free electron density ranges between  $1 \times 10^8$  and  $5 \times 10^8$  K and  $10^{26} - 10^{27} \text{ cm}^{-3}$ , respectively. In such conditions the ionization of atoms and  $\beta^-$  decay from the excited nuclear levels changes the total  $\beta^-$  decay rate noticeably. In the following sections, we discuss these effects.

### 1. Ionization of atoms: Presence of bare atoms

The probability of bound state  $\beta^-$  decay is directly related to the availability of phase space volume of the atomic shells of the parent atom. Relativistic solution of the electronic radial function indicates that bound state decay probability is highly dominated by the creation of electrons in the atomic  $K$  shell,

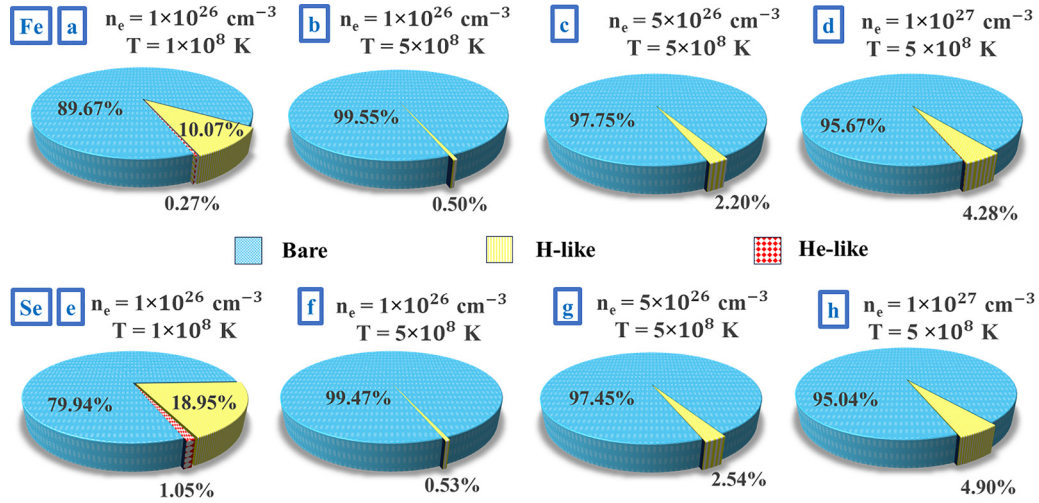


FIG. 3. Percentage of the different ionization states for Fe (upper panel) and Se (lower panel) at different free electron density ( $n_e$ ) and temperature ( $T$ ) situations.

followed by  $L$ ,  $M$ , and  $N$  shells. As a consequence, to get the bound state  $\beta^-$  decay rate it is essential to have exact information about the charge state and, more specifically, occupancies of the electronics shells of the parent atom.

In the stellar conditions mentioned above, the atoms get ionized. The charge state of the ionized atoms depends on various factors like temperature of the environment, free electron density, and ionization potential [4]. The Saha ionization equation [5] provides a clear view of the ionization scenario as a ratio of two different charge states of an atom in thermodynamic equilibrium (see Appendix C for details). It can be shown that, with the increase in temperature of the stellar site, atoms tend to be in higher and higher charge states. Whereas an increase of the free electron density inhibits the ionization of the atoms, on the other hand, in such circumstances, the ionization potential of an atom embedded in matter in thermodynamic equilibrium gets reduced. This phenomenon of reduction of the ionization potential, known as IPD, also needs to be included to get the actual ionization scenario of any stellar environment. In Fig. 3, the charge state distributions of Fe and Se atoms over a density-temperature grid are shown as examples. Interestingly, neutral atoms are totally absent, and the fully ionized charged state dominates with a few percent of H-like and He-like atoms.

We have calculated the IPDs ( $\Delta_j$ ) of the set of parent and daughter atoms, and also the charge states of those as a function of  $n_e$  and  $T$  to confirm the presence of bare atoms.

## 2. Variations of individual transition rate with temperature and density

The lowering of ionization potential (IPD) in stellar plasma [21], due to the effect of high temperature and free electron density, causes the neutral atom  $\beta^-$  decay  $Q$  value  $Q_n$  to be reduced by an amount  $\Delta Q = (\sum_{j_D=0}^{Z_D-1} \Delta_j - \sum_{j_P=0}^{Z_P-1} \Delta_j)$  as mentioned in Eq. (6). Thus  $\Delta Q$  is the IPD correction to  $Q_n$ . The left panel of Fig. 4 shows the variation of  $\Delta Q$  with temperature and density.  $\Delta Q$  decreases with temperature, and as a result the  $Q_m$  value increases, whereas the increase of  $\Delta Q$  with free electron density reduces the  $Q_m$  value. Both these variations of  $Q_m$  value are shown in the right-hand panel of Fig. 4 for the case of ground state  $\beta^-$  decay of  $^{66}\text{Ni}$ .

In Fig. 5, the variation of decay rates with temperature and density is shown, for the case of  $^{66}\text{Ni}$ . It can be observed that both bound and continuum state decay rates decrease with free electron density, since the phase space factor  $f_a^*$  of the continuum and the bound state decays are affected. The common deciding factor for this trend is the increase of IPD

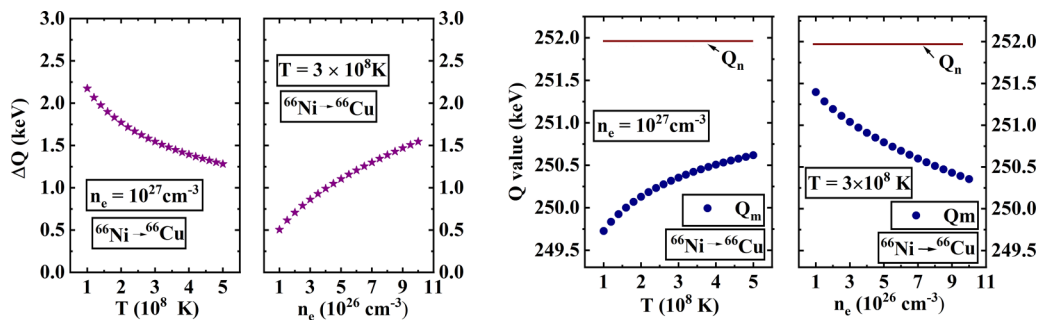


FIG. 4. Left: Variation of IPD correction  $\Delta Q = (\sum_{j_D=0}^{Z_D-1} \Delta_j - \sum_{j_P=0}^{Z_P-1} \Delta_j)$  with temperature and free electron density. Right: Variation of  $Q_m$  with temperature and free electron density, for the  $\beta^-$  decay from the ground state of  $^{66}\text{Ni}$ .

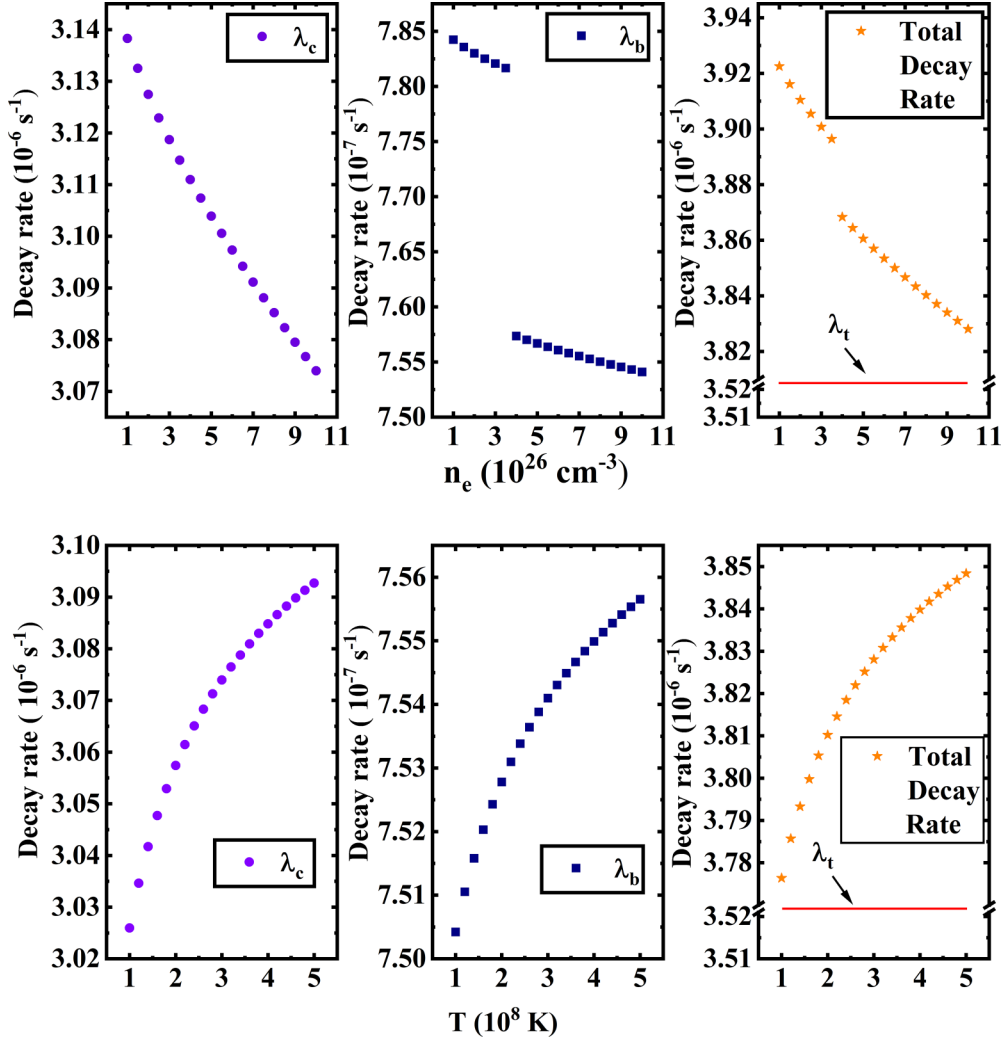


FIG. 5. Top: Variation of continuum decay rate, bound state decay rate, and total decay rate with free electron density at  $T = 3 \times 10^8 \text{ K}$ . Bottom: Variation of continuum decay rate, bound state decay rate, and total decay rate with temperature at  $n_e = 10^{27} \text{ cm}^{-3}$ , for the  $\beta^-$  decay from the ground state of  $^{66}\text{Ni}$ .  $\lambda_t$  is the terrestrial decay rate of the corresponding neutral atom. In the rightmost boxes of the top and bottom panels the y axis has been broken to include the terrestrial decay rate in the plot.

correction with increasing density which is shown in Fig. 4. In addition, in the case of decay to continuum, the factor  $(1 - f_{FD}(\eta, \beta))$  [Eq. (2)] is also responsible for the decrease of decay rate with density. However, depression of continuum results in the disappearance of atomic bound orbits. With the increase of IPD with density (as shown in Fig. 4), it is possible that the atomic  $M$  and  $N$  orbits ( $n > 2$ , where  $n$  is the principal quantum number) become unbound, and hence only  $K$  and  $L$  orbits contribute to bound state decay. This in turn generates a sudden drop of bound state decay as shown in Fig. 5.

From the lower panel of Fig. 5, it is to be noted that decay rates vary differently with temperature than with density. With an increase in temperature, the decay rates increase for both continuum state and bound state decays. Here, again the deciding factor for this variation is the variation of IPD as shown in Fig. 4. Moreover, the temperature dependence of the phase space factor, through the factor  $(1 - f_{FD}(\eta, \beta))$ , is causing an increase in continuum state decay rate with temperature.

In Table III, we show the dependence of individual transition rates, separately for  $\lambda_c$  and  $\lambda_b$  at two temperatures  $T = 10^8 \text{ K}$  and  $T = 5 \times 10^8 \text{ K}$  for the free electron density  $n_e = 10^{27} \text{ cm}^{-3}$ . Both  $\lambda_b$  and  $\lambda_c$  increase slightly with increase in temperature, for the set of nuclei of our interest.

Similarly, in Table IV, we present the dependence of individual transition rates, separately for  $\lambda_c$  and  $\lambda_b$  for two densities  $n_e = 10^{26} \text{ cm}^{-3}$  and  $n_e = 10^{27} \text{ cm}^{-3}$  at a temperature  $T = 3 \times 10^8 \text{ K}$ . Both  $\lambda_c$  and  $\lambda_b$  decrease slightly with the increasing density, for all nuclei considered here.

### 3. $\beta^-$ decay from excited nuclear levels

The equilibrium population of the thermally excited energy levels of the nuclei of interest is calculated using Boltzmann's distribution as mentioned in Sec. II B. We considered  $\beta^-$  decay only from those levels whose population is up to  $10^{-5}$  times that of the ground level.

We illustrate the contribution of excited nuclear levels to the decay rate for various density-temperature combinations

TABLE III. Bound state decay rate ( $\lambda_b$  in  $s^{-1}$ ) and continuum state decay rate ( $\lambda_c$  in  $s^{-1}$ ) variation with temperature at a free electron density  $n_e = 1 \times 10^{27} \text{ cm}^{-3}$  for each transition. There are blank spaces in columns 4 and 5 because those excited states are not populated at the corresponding temperature.

Transition details			$n_e = 1 \times 10^{27} \text{ cm}^{-3}$			
			$T = 1 \times 10^8 \text{ K}$		$T = 5 \times 10^8 \text{ K}$	
			$J_p^\pi$	$J_d^\pi$	$\lambda_c$	$\lambda_b$
$^{59}\text{Fe} \rightarrow ^{59}\text{Co}$	$3/2_1^-$	$3/2_1^-$	$8.93 \times 10^{-8}$	$7.62 \times 10^{-9}$	$9.02 \times 10^{-8}$	$7.65 \times 10^{-9}$
		$3/2_2^-$	$9.27 \times 10^{-8}$	$1.74 \times 10^{-8}$	$9.45 \times 10^{-8}$	$1.75 \times 10^{-8}$
		$1/2_1^-$	$5.46 \times 10^{-10}$	$2.85 \times 10^{-10}$	$5.70 \times 10^{-10}$	$2.88 \times 10^{-10}$
		$5/2_1^-$	$2.45 \times 10^{-11}$	$2.39 \times 10^{-11}$	$2.63 \times 10^{-11}$	$2.44 \times 10^{-11}$
	$1/2_1^-$	$3/2_1^-$			$2.60 \times 10^{-7}$	$1.01 \times 10^{-8}$
		$3/2_2^-$			$2.82 \times 10^{-7}$	$1.79 \times 10^{-8}$
		$1/2_1^-$			$5.47 \times 10^{-7}$	$5.47 \times 10^{-8}$
	$5/2_1^-$	$7/2_1^-$			$6.47 \times 10^{-4}$	$3.62 \times 10^{-6}$
		$3/2_1^-$			$1.03 \times 10^{-6}$	$2.72 \times 10^{-8}$
		$3/2_2^-$			$6.32 \times 10^{-8}$	$2.49 \times 10^{-9}$
		$5/2_1^-$			$4.98 \times 10^{-9}$	$3.19 \times 10^{-10}$
		$7/2_2^-$			$5.75 \times 10^{-8}$	$9.65 \times 10^{-9}$
$^{60}\text{Co} \rightarrow ^{60}\text{Ni}$	$5_1^+$	$4_1^+$	$6.24 \times 10^{-9}$	$1.03 \times 10^{-9}$	$6.34 \times 10^{-9}$	$1.03 \times 10^{-9}$
	$2_1^+$	$2_1^+$	$2.02 \times 10^{-6}$	$2.21 \times 10^{-8}$	$2.02 \times 10^{-6}$	$2.21 \times 10^{-8}$
		$2_2^+$	$8.97 \times 10^{-8}$	$4.08 \times 10^{-9}$	$9.03 \times 10^{-8}$	$4.09 \times 10^{-9}$
	$4_1^+$	$4_1^+$			$4.21 \times 10^{-7}$	$2.64 \times 10^{-8}$
		$3_1^+$			$4.05 \times 10^{-8}$	$3.63 \times 10^{-9}$
	$3_1^+$	$2_1^+$			$1.02 \times 10^{-5}$	$8.35 \times 10^{-8}$
		$2_2^+$			$3.85 \times 10^{-7}$	$1.08 \times 10^{-8}$
		$4_1^+$			$1.59 \times 10^{-7}$	$9.67 \times 10^{-9}$
		$3_1^+$			$3.87 \times 10^{-9}$	$3.35 \times 10^{-10}$
	$5_2^+$	$4_1^+$			$2.80 \times 10^{-7}$	$1.19 \times 10^{-8}$
$4_2^+$				$4.28 \times 10^{-10}$	$2.18 \times 10^{-10}$	
$^{61}\text{Co} \rightarrow ^{61}\text{Ni}$	$7/2_1^-$	$5/2_1^-$	$9.98 \times 10^{-5}$	$1.66 \times 10^{-6}$	$1.00 \times 10^{-4}$	$1.66 \times 10^{-6}$
		$5/2_2^-$	$3.40 \times 10^{-7}$	$3.76 \times 10^{-8}$	$3.44 \times 10^{-7}$	$3.78 \times 10^{-8}$
		$7/2_1^-$	$4.92 \times 10^{-7}$	$5.62 \times 10^{-8}$	$4.98 \times 10^{-7}$	$5.64 \times 10^{-8}$
		$7/2_2^-$	$1.31 \times 10^{-7}$	$2.25 \times 10^{-8}$	$1.34 \times 10^{-7}$	$2.26 \times 10^{-8}$
		$5/2_3^-$	$1.39 \times 10^{-7}$	$4.66 \times 10^{-8}$	$1.43 \times 10^{-7}$	$4.70 \times 10^{-8}$
$^{63}\text{Ni} \rightarrow ^{63}\text{Cu}$	$1/2_1^-$	$3/2_1^-$	$3.50 \times 10^{-10}$	$5.72 \times 10^{-10}$	$3.84 \times 10^{-10}$	$5.86 \times 10^{-10}$
	$5/2_1^-$	$3/2_1^-$	$2.13 \times 10^{-8}$	$1.04 \times 10^{-8}$	$2.21 \times 10^{-8}$	$1.06 \times 10^{-8}$
$^{65}\text{Ni} \rightarrow ^{65}\text{Cu}$	$3/2_1^-$	$3/2_1^-$			$1.97 \times 10^{-7}$	$5.72 \times 10^{-8}$
	$5/2_1^-$	$3/2_1^-$	$4.50 \times 10^{-5}$	$2.71 \times 10^{-7}$	$4.51 \times 10^{-5}$	$2.72 \times 10^{-7}$
		$5/2_1^-$	$3.58 \times 10^{-6}$	$9.57 \times 10^{-8}$	$3.59 \times 10^{-6}$	$9.58 \times 10^{-8}$
		$7/2_1^-$	$2.02 \times 10^{-5}$	$1.18 \times 10^{-6}$	$2.04 \times 10^{-5}$	$1.18 \times 10^{-6}$
		$5/2_2^-$	$1.78 \times 10^{-6}$	$1.53 \times 10^{-7}$	$1.80 \times 10^{-6}$	$1.54 \times 10^{-7}$
		$3/2_2^-$	$1.42 \times 10^{-7}$	$1.72 \times 10^{-8}$	$1.44 \times 10^{-7}$	$1.73 \times 10^{-8}$
		$7/2_2^-$	$2.38 \times 10^{-9}$	$7.90 \times 10^{-9}$	$2.75 \times 10^{-9}$	$8.19 \times 10^{-9}$
		$5/2_3^-$	$1.21 \times 10^{-12}$	$8.00 \times 10^{-12}$	$1.49 \times 10^{-12}$	$8.41 \times 10^{-12}$
$1/2_1^-$	$3/2_1^-$	$5.39 \times 10^{-3}$	$3.05 \times 10^{-5}$	$5.40 \times 10^{-3}$	$3.05 \times 10^{-5}$	
	$1/2_1^-$	$2.38 \times 10^{-5}$	$3.33 \times 10^{-7}$	$2.38 \times 10^{-5}$	$3.33 \times 10^{-7}$	
	$3/2_2^-$	$3.10 \times 10^{-7}$	$3.01 \times 10^{-8}$	$3.13 \times 10^{-7}$	$3.02 \times 10^{-8}$	
$^{66}\text{Ni} \rightarrow ^{66}\text{Cu}$	$0_1^+$	$1_1^+$	$3.03 \times 10^{-6}$	$7.50 \times 10^{-7}$	$3.09 \times 10^{-6}$	$7.55 \times 10^{-7}$
$^{64}\text{Cu} \rightarrow ^{64}\text{Zn}$	$1_1^+$	$0_1^+$	$4.95 \times 10^{-6}$	$3.81 \times 10^{-7}$	$5.00 \times 10^{-6}$	$3.83 \times 10^{-7}$
$^{66}\text{Cu} \rightarrow ^{66}\text{Zn}$	$1_1^+$	$0_1^+$	$1.19 \times 10^{-3}$	$4.85 \times 10^{-6}$	$1.19 \times 10^{-3}$	$4.85 \times 10^{-6}$
		$2_1^+$	$3.48 \times 10^{-4}$	$4.21 \times 10^{-6}$	$3.49 \times 10^{-4}$	$4.21 \times 10^{-6}$
		$2_2^+$	$2.17 \times 10^{-6}$	$1.04 \times 10^{-7}$	$2.18 \times 10^{-6}$	$1.05 \times 10^{-7}$
		$0_2^+$	$2.19 \times 10^{-8}$	$5.35 \times 10^{-9}$	$2.23 \times 10^{-8}$	$5.38 \times 10^{-9}$



TABLE III. (Continued.)

Transition details			$n_e = 1 \times 10^{27} \text{ cm}^{-3}$			
			$T = 1 \times 10^8 \text{ K}$		$T = 5 \times 10^8 \text{ K}$	
Decay	$J_p^\pi$	$J_d^\pi$	$\lambda_c$	$\lambda_b$	$\lambda_c$	$\lambda_b$
$^{67}\text{Cu} \rightarrow ^{67}\text{Zn}$	$3/2_1^-$	$5/2_1^-$	$1.09 \times 10^{-6}$	$8.83 \times 10^{-8}$	$1.10 \times 10^{-6}$	$8.86 \times 10^{-8}$
		$1/2_1^-$	$5.72 \times 10^{-7}$	$6.16 \times 10^{-8}$	$5.79 \times 10^{-7}$	$6.19 \times 10^{-8}$
		$3/2_1^-$	$9.45 \times 10^{-7}$	$1.41 \times 10^{-7}$	$9.58 \times 10^{-7}$	$1.42 \times 10^{-7}$
$^{69}\text{Zn} \rightarrow ^{69}\text{Ga}$	$1/2_1^-$	$3/2_2^-$	$4.85 \times 10^{-8}$	$2.28 \times 10^{-8}$	$5.02 \times 10^{-8}$	$2.31 \times 10^{-8}$
		$3/2_1^-$	$2.09 \times 10^{-4}$	$8.07 \times 10^{-6}$	$2.10 \times 10^{-4}$	$8.09 \times 10^{-6}$
		$1/2_1^-$	$2.88 \times 10^{-8}$	$2.31 \times 10^{-9}$	$2.91 \times 10^{-8}$	$2.32 \times 10^{-9}$
$^{72}\text{Zn} \rightarrow ^{72}\text{Ga}$	$0_1^+$	$3/2_2^-$	$4.07 \times 10^{-10}$	$2.11 \times 10^{-9}$	$4.83 \times 10^{-10}$	$2.20 \times 10^{-9}$
		$0_1^+$	$7.50 \times 10^{-9}$	$1.34 \times 10^{-9}$	$7.63 \times 10^{-9}$	$1.52 \times 10^{-9}$
		$1_1^+$	$2.07 \times 10^{-6}$	$4.35 \times 10^{-7}$	$2.11 \times 10^{-6}$	$4.37 \times 10^{-7}$
		$1_2^+$	$2.08 \times 10^{-6}$	$5.12 \times 10^{-7}$	$2.12 \times 10^{-6}$	$5.15 \times 10^{-7}$
$^{70}\text{Ga} \rightarrow ^{70}\text{Ge}$	$1_1^+$	$1_3^+$	$1.13 \times 10^{-6}$	$3.60 \times 10^{-7}$	$1.16 \times 10^{-6}$	$3.62 \times 10^{-7}$
		$0_1^+$	$5.22 \times 10^{-4}$	$6.93 \times 10^{-6}$	$5.24 \times 10^{-4}$	$6.94 \times 10^{-6}$
		$2_1^+$	$1.38 \times 10^{-5}$	$1.13 \times 10^{-6}$	$1.39 \times 10^{-5}$	$1.13 \times 10^{-6}$
$^{75}\text{Ge} \rightarrow ^{75}\text{As}$	$1/2_1^-$	$0_2^+$	$1.87 \times 10^{-6}$	$2.60 \times 10^{-7}$	$1.89 \times 10^{-6}$	$2.61 \times 10^{-7}$
		$3/2_1^-$	$1.21 \times 10^{-4}$	$3.38 \times 10^{-6}$	$1.22 \times 10^{-4}$	$3.39 \times 10^{-6}$
		$1/2_1^-$	$6.25 \times 10^{-7}$	$2.45 \times 10^{-8}$	$6.28 \times 10^{-7}$	$2.46 \times 10^{-8}$
		$3/2_2^-$	$1.57 \times 10^{-5}$	$7.00 \times 10^{-7}$	$1.58 \times 10^{-5}$	$7.02 \times 10^{-7}$
		$1/2_2^-$	$2.26 \times 10^{-7}$	$1.55 \times 10^{-8}$	$2.27 \times 10^{-7}$	$1.56 \times 10^{-8}$
		$1/2_3^-$	$4.74 \times 10^{-6}$	$4.38 \times 10^{-7}$	$4.78 \times 10^{-6}$	$4.39 \times 10^{-7}$
		$3/2_3^-$	$6.63 \times 10^{-7}$	$6.71 \times 10^{-8}$	$6.69 \times 10^{-7}$	$6.73 \times 10^{-8}$
		$3/2_4^-$	$6.99 \times 10^{-9}$	$1.71 \times 10^{-9}$	$7.12 \times 10^{-9}$	$1.72 \times 10^{-9}$
		$3/2_5^-$	$8.09 \times 10^{-12}$	$8.30 \times 10^{-12}$	$8.56 \times 10^{-12}$	$8.44 \times 10^{-12}$
		$3/2_6^-$	$3.49 \times 10^{-10}$	$4.18 \times 10^{-10}$	$3.72 \times 10^{-10}$	$4.25 \times 10^{-10}$
		$1/2_4^-$	$2.96 \times 10^{-11}$	$1.14 \times 10^{-10}$	$3.39 \times 10^{-11}$	$1.18 \times 10^{-10}$
		$1/2_5^-$		$6.13 \times 10^{-11}$		$7.09 \times 10^{-11}$
		$7/2_1^+$	$9/2_1^+$			$3.99 \times 10^{-7}$
$5/2_1^+$				$5.75 \times 10^{-7}$	$2.53 \times 10^{-8}$	
$5/2_2^+$				$6.59 \times 10^{-8}$	$2.36 \times 10^{-8}$	
$5/2_3^+$				$6.66 \times 10^{-9}$	$2.68 \times 10^{-9}$	
$9/2_2^+$				$1.42 \times 10^{-10}$	$4.13 \times 10^{-10}$	
$3/2_1^-$	$5/2_4^+$			$1.84 \times 10^{-12}$	$1.33 \times 10^{-10}$	
	$3/2_1^-$	$3/2_1^-$		$7.46 \times 10^{-5}$	$1.42 \times 10^{-6}$	
	$1/2_1^-$	$1/2_1^-$		$3.52 \times 10^{-5}$	$8.97 \times 10^{-7}$	
	$3/2_2^-$	$3/2_2^-$		$9.71 \times 10^{-6}$	$2.75 \times 10^{-7}$	
	$5/2_1^-$	$5/2_1^-$		$1.85 \times 10^{-7}$	$5.37 \times 10^{-9}$	
	$1/2_2^-$	$1/2_2^-$		$1.11 \times 10^{-7}$	$4.49 \times 10^{-9}$	
	$5/2_2^-$	$5/2_2^-$		$6.76 \times 10^{-7}$	$3.34 \times 10^{-8}$	
	$1/2_3^-$	$1/2_3^-$		$2.69 \times 10^{-7}$	$1.36 \times 10^{-8}$	
	$3/2_3^-$	$3/2_3^-$		$1.18 \times 10^{-6}$	$6.42 \times 10^{-8}$	
	$3/2_4^-$	$3/2_4^-$		$3.79 \times 10^{-7}$	$3.75 \times 10^{-8}$	
	$3/2_5^-$	$3/2_5^-$		$2.21 \times 10^{-7}$	$4.23 \times 10^{-8}$	
	$3/2_6^-$	$3/2_6^-$		$1.57 \times 10^{-8}$	$3.15 \times 10^{-9}$	
	$1/2_4^-$	$1/2_4^-$		$2.46 \times 10^{-8}$	$6.18 \times 10^{-9}$	
	$1/2_5^-$	$1/2_5^-$		$1.43 \times 10^{-8}$	$4.53 \times 10^{-9}$	
	$3/2_7^-$	$3/2_7^-$		$1.55 \times 10^{-8}$	$5.88 \times 10^{-9}$	
$3/2_8^-$	$3/2_8^-$		$2.83 \times 10^{-10}$	$4.58 \times 10^{-10}$		
$3/2_9^-$	$3/2_9^-$		$5.29 \times 10^{-10}$	$1.38 \times 10^{-9}$		
$5/2_3^-$	$5/2_3^-$		$2.73 \times 10^{-13}$	$1.08 \times 10^{-10}$		
$^{78}\text{Ge} \rightarrow ^{78}\text{As}$	$0_1^+$	$1_1^+$	$5.21 \times 10^{-5}$	$3.86 \times 10^{-6}$	$5.25 \times 10^{-5}$	$3.87 \times 10^{-6}$
		$1_2^+$	$1.89 \times 10^{-5}$	$1.46 \times 10^{-6}$	$1.91 \times 10^{-5}$	$1.47 \times 10^{-6}$
		$1_3^+$	$5.57 \times 10^{-5}$	$8.82 \times 10^{-6}$	$5.65 \times 10^{-5}$	$8.86 \times 10^{-6}$
$^{81}\text{Se} \rightarrow ^{81}\text{Br}$	$1/2_1^-$	$3/2_1^-$	$5.77 \times 10^{-4}$	$1.03 \times 10^{-5}$	$5.79 \times 10^{-4}$	$1.03 \times 10^{-5}$

TABLE III. (Continued.)

Transition details			$n_e = 1 \times 10^{27} \text{ cm}^{-3}$			
			$T = 1 \times 10^8 \text{ K}$		$T = 5 \times 10^8 \text{ K}$	
Decay	$J_p^\pi$	$J_d^\pi$	$\lambda_c$	$\lambda_b$	$\lambda_c$	$\lambda_b$
		$1/2_1^-$	$1.40 \times 10^{-7}$	$5.56 \times 10^{-9}$	$1.41 \times 10^{-7}$	$5.57 \times 10^{-9}$
		$3/2_2^-$	$5.77 \times 10^{-7}$	$2.41 \times 10^{-8}$	$5.80 \times 10^{-7}$	$2.41 \times 10^{-8}$
		$3/2_3^-$	$1.04 \times 10^{-6}$	$5.05 \times 10^{-8}$	$1.04 \times 10^{-6}$	$5.06 \times 10^{-8}$
		$3/2_4^-$	$5.07 \times 10^{-6}$	$3.57 \times 10^{-7}$	$5.11 \times 10^{-6}$	$3.58 \times 10^{-7}$
		$1/2_2^-$	$1.74 \times 10^{-7}$	$2.55 \times 10^{-8}$	$1.76 \times 10^{-7}$	$2.56 \times 10^{-8}$
		$3/2_5^-$	$1.80 \times 10^{-8}$	$4.85 \times 10^{-9}$	$1.83 \times 10^{-8}$	$4.88 \times 10^{-9}$
		$3/2_6^-$	$4.41 \times 10^{-11}$	$2.12 \times 10^{-10}$	$5.09 \times 10^{-11}$	$2.20 \times 10^{-10}$
		$3/2_7^-$	$7.02 \times 10^{-11}$	$4.64 \times 10^{-10}$	$8.31 \times 10^{-11}$	$4.84 \times 10^{-10}$

TABLE IV. Bound state decay rate ( $\lambda_b$  in  $\text{s}^{-1}$ ) and continuum state decay rate ( $\lambda_c$  in  $\text{s}^{-1}$ ) variation with free electron density at a temperature  $T = 3 \times 10^8 \text{ K}$  for each transition. This table does not include the levels that are not populated at this temperature.

Transition details			$T = 3 \times 10^8 \text{ K}$			
			$n_e = 1 \times 10^{26} \text{ cm}^{-3}$		$n_e = 1 \times 10^{27} \text{ cm}^{-3}$	
Decay	$J_p^\pi$	$J_d^\pi$	$\lambda_c$	$\lambda_b$	$\lambda_c$	$\lambda_b$
$^{59}\text{Fe} \rightarrow ^{59}\text{Co}$	$3/2_1^-$	$3/2_1^-$	$9.09 \times 10^{-8}$	$7.92 \times 10^{-9}$	$8.99 \times 10^{-8}$	$7.64 \times 10^{-9}$
		$3/2_2^-$	$9.57 \times 10^{-8}$	$1.81 \times 10^{-8}$	$9.40 \times 10^{-8}$	$1.75 \times 10^{-8}$
		$1/2_1^-$	$5.85 \times 10^{-10}$	$3.00 \times 10^{-10}$	$5.64 \times 10^{-10}$	$2.87 \times 10^{-10}$
$^{60}\text{Co} \rightarrow ^{60}\text{Ni}$	$5_1^+$	$5/2_1^-$	$2.73 \times 10^{-11}$	$2.55 \times 10^{-11}$	$2.58 \times 10^{-11}$	$2.43 \times 10^{-11}$
		$4_1^+$	$6.41 \times 10^{-9}$	$1.07 \times 10^{-9}$	$6.31 \times 10^{-9}$	$1.03 \times 10^{-9}$
		$2_1^+$	$2.03 \times 10^{-6}$	$2.29 \times 10^{-8}$	$2.02 \times 10^{-6}$	$2.21 \times 10^{-8}$
$^{61}\text{Co} \rightarrow ^{61}\text{Ni}$	$7/2_1^-$	$2_2^+$	$9.07 \times 10^{-8}$	$4.24 \times 10^{-9}$	$9.01 \times 10^{-8}$	$4.09 \times 10^{-9}$
		$4_1^+$	$4.23 \times 10^{-7}$	$2.73 \times 10^{-8}$	$4.20 \times 10^{-7}$	$2.64 \times 10^{-8}$
		$3_1^+$	$4.08 \times 10^{-8}$	$3.76 \times 10^{-9}$	$4.03 \times 10^{-8}$	$3.63 \times 10^{-9}$
		$5/2_1^-$	$1.00 \times 10^{-4}$	$1.72 \times 10^{-6}$	$1.00 \times 10^{-4}$	$1.66 \times 10^{-6}$
		$5/2_2^-$	$3.47 \times 10^{-7}$	$3.91 \times 10^{-8}$	$3.43 \times 10^{-7}$	$3.77 \times 10^{-8}$
$^{63}\text{Ni} \rightarrow ^{63}\text{Cu}$	$1/2_1^-$	$7/2_1^-$	$5.02 \times 10^{-7}$	$5.85 \times 10^{-8}$	$4.96 \times 10^{-7}$	$5.64 \times 10^{-8}$
		$7/2_2^-$	$1.35 \times 10^{-7}$	$2.35 \times 10^{-8}$	$1.33 \times 10^{-7}$	$2.26 \times 10^{-8}$
		$5/2_3^-$	$1.46 \times 10^{-7}$	$4.88 \times 10^{-8}$	$1.43 \times 10^{-7}$	$4.69 \times 10^{-8}$
		$3/2_1^-$	$4.03 \times 10^{-10}$	$6.14 \times 10^{-10}$	$3.76 \times 10^{-10}$	$5.82 \times 10^{-10}$
$^{65}\text{Ni} \rightarrow ^{65}\text{Cu}$	$5/2_1^-$	$5/2_1^-$	$2.26 \times 10^{-8}$	$1.10 \times 10^{-8}$	$2.19 \times 10^{-8}$	$1.05 \times 10^{-8}$
		$3/2_1^-$	$2.00 \times 10^{-7}$	$5.94 \times 10^{-8}$	$1.96 \times 10^{-7}$	$5.70 \times 10^{-8}$
		$5/2_1^-$	$4.52 \times 10^{-5}$	$2.81 \times 10^{-7}$	$4.51 \times 10^{-5}$	$2.71 \times 10^{-7}$
		$7/2_1^-$	$3.60 \times 10^{-6}$	$9.92 \times 10^{-8}$	$3.59 \times 10^{-6}$	$9.58 \times 10^{-8}$
		$7/2_1^-$	$2.05 \times 10^{-5}$	$1.22 \times 10^{-6}$	$2.03 \times 10^{-5}$	$1.18 \times 10^{-6}$
		$5/2_2^-$	$1.81 \times 10^{-6}$	$1.59 \times 10^{-7}$	$1.79 \times 10^{-6}$	$1.54 \times 10^{-7}$
		$3/2_2^-$	$1.45 \times 10^{-7}$	$1.79 \times 10^{-8}$	$1.43 \times 10^{-7}$	$1.72 \times 10^{-8}$
		$7/2_2^-$	$2.95 \times 10^{-9}$	$8.64 \times 10^{-9}$	$2.66 \times 10^{-9}$	$8.11 \times 10^{-9}$
$^{66}\text{Ni} \rightarrow ^{66}\text{Cu}$	$1/2_1^-$	$5/2_3^-$	$1.65 \times 10^{-12}$	$8.93 \times 10^{-12}$	$1.42 \times 10^{-12}$	$8.28 \times 10^{-12}$
		$3/2_1^-$	$5.41 \times 10^{-3}$	$3.15 \times 10^{-5}$	$5.40 \times 10^{-3}$	$3.05 \times 10^{-5}$
		$1/2_1^-$	$2.39 \times 10^{-5}$	$3.45 \times 10^{-7}$	$2.38 \times 10^{-5}$	$3.33 \times 10^{-7}$
$^{64}\text{Cu} \rightarrow ^{64}\text{Zn}$	$1_1^+$	$3/2_2^-$	$3.16 \times 10^{-7}$	$3.13 \times 10^{-8}$	$3.12 \times 10^{-7}$	$3.02 \times 10^{-8}$
		$0_1^+$	$3.14 \times 10^{-6}$	$7.84 \times 10^{-7}$	$3.07 \times 10^{-6}$	$7.54 \times 10^{-7}$
$^{66}\text{Cu} \rightarrow ^{66}\text{Zn}$	$1_1^+$	$0_1^+$	$5.03 \times 10^{-6}$	$3.96 \times 10^{-7}$	$4.98 \times 10^{-6}$	$3.82 \times 10^{-7}$
		$2_1^+$	$1.19 \times 10^{-3}$	$5.02 \times 10^{-6}$	$1.19 \times 10^{-3}$	$4.85 \times 10^{-6}$
		$2_2^+$	$3.50 \times 10^{-4}$	$4.36 \times 10^{-6}$	$3.49 \times 10^{-4}$	$4.21 \times 10^{-6}$
		$2_2^+$	$2.19 \times 10^{-6}$	$1.08 \times 10^{-7}$	$2.18 \times 10^{-6}$	$1.05 \times 10^{-7}$

TABLE IV. (Continued.)

Transition details			$T = 3 \times 10^8 \text{ K}$				
			$n_e = 1 \times 10^{26} \text{ cm}^{-3}$		$n_e = 1 \times 10^{27} \text{ cm}^{-3}$		
			$\lambda_c$	$\lambda_b$	$\lambda_c$	$\lambda_b$	
Decay	$J_p^\pi$	$J_d^\pi$					
$^{67}\text{Cu} \rightarrow ^{67}\text{Zn}$	$3/2_1^-$	$0_2^+$	$2.26 \times 10^{-8}$	$5.58 \times 10^{-9}$	$2.22 \times 10^{-8}$	$5.37 \times 10^{-9}$	
		$5/2_1^-$	$1.11 \times 10^{-6}$	$9.18 \times 10^{-8}$	$1.10 \times 10^{-6}$	$8.85 \times 10^{-8}$	
		$1/2_1^-$	$5.83 \times 10^{-7}$	$6.41 \times 10^{-8}$	$5.77 \times 10^{-7}$	$6.18 \times 10^{-8}$	
$^{69}\text{Zn} \rightarrow ^{69}\text{Ga}$	$1/2_1^-$	$3/2_1^-$	$9.68 \times 10^{-7}$	$1.47 \times 10^{-7}$	$9.54 \times 10^{-7}$	$1.42 \times 10^{-7}$	
		$3/2_2^-$	$5.13 \times 10^{-8}$	$2.40 \times 10^{-8}$	$4.97 \times 10^{-8}$	$2.30 \times 10^{-8}$	
		$3/2_1^-$	$2.11 \times 10^{-4}$	$8.38 \times 10^{-6}$	$2.10 \times 10^{-4}$	$8.09 \times 10^{-6}$	
$^{72}\text{Zn} \rightarrow ^{72}\text{Ga}$	$0_1^+$	$1/2_1^-$	$2.92 \times 10^{-8}$	$2.40 \times 10^{-9}$	$2.90 \times 10^{-8}$	$2.32 \times 10^{-9}$	
		$3/2_2^-$	$5.26 \times 10^{-10}$	$2.33 \times 10^{-9}$	$4.64 \times 10^{-10}$	$2.18 \times 10^{-9}$	
		$0_1^+$	$7.72 \times 10^{-9}$	$1.58 \times 10^{-9}$	$7.59 \times 10^{-9}$	$1.52 \times 10^{-9}$	
$^{70}\text{Ga} \rightarrow ^{70}\text{Ge}$	$1_1^+$	$1_1^+$	$2.13 \times 10^{-6}$	$4.54 \times 10^{-7}$	$2.10 \times 10^{-6}$	$4.37 \times 10^{-7}$	
		$1_2^+$	$2.15 \times 10^{-6}$	$5.35 \times 10^{-7}$	$2.11 \times 10^{-6}$	$5.14 \times 10^{-7}$	
		$1_3^+$	$1.18 \times 10^{-6}$	$3.76 \times 10^{-7}$	$1.15 \times 10^{-6}$	$3.61 \times 10^{-7}$	
$^{75}\text{Ge} \rightarrow ^{75}\text{As}$	$1/2_1^-$	$0_1^+$	$5.25 \times 10^{-4}$	$7.18 \times 10^{-6}$	$5.23 \times 10^{-4}$	$6.94 \times 10^{-6}$	
		$2_1^+$	$1.40 \times 10^{-5}$	$1.17 \times 10^{-6}$	$1.39 \times 10^{-5}$	$1.13 \times 10^{-6}$	
		$0_2^+$	$1.91 \times 10^{-6}$	$2.71 \times 10^{-7}$	$1.89 \times 10^{-6}$	$2.61 \times 10^{-7}$	
$^{75}\text{Ge} \rightarrow ^{75}\text{As}$	$1/2_1^-$	$3/2_1^-$	$1.22 \times 10^{-4}$	$3.51 \times 10^{-6}$	$1.22 \times 10^{-4}$	$3.38 \times 10^{-6}$	
		$1/2_1^-$	$6.31 \times 10^{-7}$	$2.54 \times 10^{-8}$	$6.27 \times 10^{-7}$	$2.46 \times 10^{-8}$	
		$3/2_2^-$	$1.59 \times 10^{-5}$	$7.27 \times 10^{-7}$	$1.58 \times 10^{-5}$	$7.01 \times 10^{-7}$	
		$1/2_2^-$	$2.29 \times 10^{-7}$	$1.61 \times 10^{-8}$	$2.27 \times 10^{-7}$	$1.56 \times 10^{-8}$	
		$1/2_3^-$	$4.81 \times 10^{-7}$	$4.55 \times 10^{-7}$	$4.77 \times 10^{-6}$	$4.39 \times 10^{-7}$	
		$3/2_3^-$	$6.74 \times 10^{-7}$	$6.97 \times 10^{-8}$	$6.67 \times 10^{-7}$	$6.72 \times 10^{-8}$	
		$3/2_4^-$	$7.21 \times 10^{-9}$	$1.78 \times 10^{-9}$	$7.08 \times 10^{-9}$	$1.72 \times 10^{-9}$	
		$3/2_5^-$	$8.85 \times 10^{-12}$	$8.80 \times 10^{-12}$	$8.43 \times 10^{-12}$	$8.40 \times 10^{-12}$	
		$3/2_6^-$	$3.86 \times 10^{-10}$	$4.44 \times 10^{-10}$	$3.66 \times 10^{-10}$	$4.23 \times 10^{-10}$	
		$1/2_4^-$	$3.63 \times 10^{-11}$	$1.24 \times 10^{-10}$	$3.28 \times 10^{-11}$	$1.17 \times 10^{-10}$	
		$1/2_5^-$	$5.35 \times 10^{-17}$	$8.02 \times 10^{-11}$		$6.80 \times 10^{-11}$	
		$7/2_1^+$	$9/2_1^+$	$4.01 \times 10^{-7}$	$1.52 \times 10^{-8}$	$3.98 \times 10^{-7}$	$1.47 \times 10^{-8}$
			$5/2_1^+$	$5.78 \times 10^{-7}$	$2.62 \times 10^{-8}$	$5.75 \times 10^{-7}$	$2.53 \times 10^{-8}$
			$5/2_2^+$	$6.71 \times 10^{-8}$	$2.45 \times 10^{-8}$	$6.54 \times 10^{-8}$	$2.35 \times 10^{-8}$
			$5/2_3^+$	$6.78 \times 10^{-9}$	$2.79 \times 10^{-9}$	$6.60 \times 10^{-9}$	$2.68 \times 10^{-9}$
$9/2_2^+$	$1.52 \times 10^{-10}$		$4.34 \times 10^{-10}$	$1.38 \times 10^{-10}$	$4.09 \times 10^{-10}$		
$5/2_4^+$	$2.49 \times 10^{-12}$		$1.44 \times 10^{-10}$	$1.63 \times 10^{-12}$	$1.29 \times 10^{-10}$		
$3/2_1^-$	$3/2_1^-$	$7.48 \times 10^{-5}$	$1.47 \times 10^{-6}$	$7.45 \times 10^{-5}$	$1.42 \times 10^{-6}$		
	$1/2_1^-$	$3.53 \times 10^{-5}$	$9.29 \times 10^{-7}$	$3.51 \times 10^{-5}$	$8.97 \times 10^{-7}$		
	$3/2_2^-$	$9.74 \times 10^{-6}$	$2.85 \times 10^{-7}$	$9.70 \times 10^{-6}$	$2.75 \times 10^{-7}$		
	$5/2_1^-$	$1.86 \times 10^{-7}$	$5.56 \times 10^{-9}$	$1.85 \times 10^{-7}$	$5.37 \times 10^{-9}$		
	$1/2_2^-$	$1.12 \times 10^{-7}$	$4.65 \times 10^{-9}$	$1.11 \times 10^{-7}$	$4.49 \times 10^{-9}$		
	$5/2_2^-$	$6.80 \times 10^{-7}$	$3.46 \times 10^{-8}$	$6.75 \times 10^{-7}$	$3.34 \times 10^{-8}$		
	$1/2_3^-$	$2.71 \times 10^{-7}$	$1.41 \times 10^{-8}$	$2.69 \times 10^{-7}$	$1.36 \times 10^{-8}$		
	$3/2_3^-$	$1.19 \times 10^{-6}$	$6.65 \times 10^{-8}$	$1.18 \times 10^{-6}$	$6.41 \times 10^{-8}$		
	$3/2_4^-$	$3.82 \times 10^{-7}$	$3.89 \times 10^{-8}$	$3.78 \times 10^{-7}$	$3.75 \times 10^{-8}$		
	$3/2_5^-$	$2.24 \times 10^{-7}$	$4.38 \times 10^{-8}$	$2.20 \times 10^{-7}$	$4.22 \times 10^{-8}$		
	$3/2_6^-$	$1.59 \times 10^{-8}$	$3.26 \times 10^{-9}$	$1.57 \times 10^{-8}$	$3.14 \times 10^{-9}$		
	$1/2_4^-$	$2.49 \times 10^{-8}$	$6.42 \times 10^{-9}$	$2.45 \times 10^{-8}$	$6.17 \times 10^{-9}$		
	$1/2_5^-$	$1.46 \times 10^{-8}$	$4.70 \times 10^{-9}$	$1.43 \times 10^{-8}$	$4.52 \times 10^{-9}$		
	$3/2_7^-$	$1.58 \times 10^{-8}$	$6.11 \times 10^{-9}$	$1.54 \times 10^{-8}$	$5.86 \times 10^{-9}$		
	$3/2_8^-$	$2.96 \times 10^{-10}$	$4.79 \times 10^{-10}$	$2.77 \times 10^{-10}$	$4.55 \times 10^{-10}$		
$3/2_9^-$	$5.61 \times 10^{-10}$	$1.45 \times 10^{-9}$	$5.14 \times 10^{-10}$	$1.37 \times 10^{-9}$			
$5/2_3^-$	$4.86 \times 10^{-13}$	$1.19 \times 10^{-10}$	$2.16 \times 10^{-13}$	$1.05 \times 10^{-10}$			
$^{78}\text{Ge} \rightarrow ^{78}\text{As}$	$0_1^+$	$1_1^+$	$5.28 \times 10^{-5}$	$4.01 \times 10^{-6}$	$5.24 \times 10^{-5}$	$3.87 \times 10^{-6}$	
		$1_2^+$	$1.92 \times 10^{-5}$	$1.52 \times 10^{-6}$	$1.91 \times 10^{-5}$	$1.47 \times 10^{-6}$	
		$1_3^+$	$5.70 \times 10^{-5}$	$9.19 \times 10^{-6}$	$5.62 \times 10^{-5}$	$8.85 \times 10^{-6}$	

TABLE IV. (Continued.)

Transition details			$T = 3 \times 10^8 \text{ K}$			
			$n_e = 1 \times 10^{26} \text{ cm}^{-3}$		$n_e = 1 \times 10^{27} \text{ cm}^{-3}$	
			$\lambda_c$	$\lambda_b$	$\lambda_c$	$\lambda_b$
$^{81}\text{Se} \rightarrow ^{81}\text{Br}$	$J_p^\pi$	$J_d^\pi$				
	$1/2_1^-$	$3/2_1^-$	$5.80 \times 10^{-4}$	$1.07 \times 10^{-5}$	$5.78 \times 10^{-4}$	$1.03 \times 10^{-5}$
		$1/2_1^-$	$1.41 \times 10^{-7}$	$5.77 \times 10^{-9}$	$1.40 \times 10^{-7}$	$5.56 \times 10^{-9}$
		$3/2_2^-$	$5.82 \times 10^{-7}$	$2.50 \times 10^{-8}$	$5.79 \times 10^{-7}$	$2.41 \times 10^{-8}$
		$3/2_3^-$	$1.05 \times 10^{-6}$	$5.25 \times 10^{-8}$	$1.04 \times 10^{-6}$	$5.06 \times 10^{-8}$
		$3/2_4^-$	$5.14 \times 10^{-6}$	$3.71 \times 10^{-7}$	$5.10 \times 10^{-6}$	$3.58 \times 10^{-7}$
		$1/2_2^-$	$1.78 \times 10^{-7}$	$2.66 \times 10^{-8}$	$1.75 \times 10^{-7}$	$2.56 \times 10^{-8}$
		$3/2_5^-$	$1.85 \times 10^{-8}$	$5.07 \times 10^{-9}$	$1.82 \times 10^{-8}$	$4.88 \times 10^{-9}$
		$3/2_6^-$	$5.50 \times 10^{-11}$	$2.31 \times 10^{-10}$	$4.92 \times 10^{-11}$	$2.17 \times 10^{-10}$
	$3/2_7^-$	$9.09 \times 10^{-11}$	$5.11 \times 10^{-10}$	$7.99 \times 10^{-11}$	$4.78 \times 10^{-10}$	

in Table V. Owing to the population of the higher energy levels of the parent, decay from these levels starts to contribute as temperature rises at a fixed density. As a result, one can see how the  $\beta$  branching ( $I_{k(gs)}$ ) from the parent's ground state (gs) decreases as the temperature rises. When we choose a larger density, the situation remains almost unaffected. Additionally, the table also includes the  $\beta$  branching ( $I_m$ ) to each daughter level for the two different densities. The branching to the daughter levels decreases with an increase in temperature in the case of a transition from the parent ground state because the parent ground state loses equilibrium population to some extent. Although branching to each daughter level increases with temperature in the case of decay from excited levels.

We use the example of  $^{59}\text{Fe}$  decaying to  $^{59}\text{Co}$  in a stellar situation to demonstrate the significance of  $\beta^-$  decay from excited levels. From the Boltzmann distribution [Eq. (13)], it was found that the populations of the higher energy levels will be considerable only at  $T \approx 5 \times 10^8 \text{ K}$ , for this particular nucleus. Terrestrially the ground state  $[0.0, 3/2^-]$  of  $^{59}\text{Fe}$  decays to four different levels:  $[1099.3, 3/2^-]$ ,  $[1291.6, 3/2^-]$ ,  $[1434.3, 1/2^-]$ , and  $[1481.6, 5/2^-]$  of  $^{59}\text{Co}$  (Fig. 6). Branching of the decay to these four levels is almost 100%. But, at this temperature, the first  $[287, 1/2^-]$  and second  $[472.9, 5/2^-]$  excited states of  $^{59}\text{Fe}$  get populated adequately. Now, these two levels can decay to various levels of the

daughter as shown in Fig. 7. In the total  $\beta^-$  decay of the parent nucleus, decay from the second excited state of the parent also contributes a substantial amount, followed by the first excited state. So we have taken into account the contribution of the excited states to bound and continuum decay for all relevant cases.

In this paper we have shown the data [Tables III–VII] only for those excited levels of parent which have contribution  $>0.1\%$ , with respect to total decay rate. However, in Table VIII, we have given the total decay rate taking into account all of the transitions. One may find the remaining data in the Supplemental Material of this paper [26].

#### 4. Contribution of bound state $\beta^-$ decay to the total $\beta^-$ decay rate

For all the terrestrially known transitions and transitions from the excited levels of the nuclei listed in Table I, we have calculated the continuum ( $\lambda_c$ ) and bound state ( $\lambda_b$ ) decay rates. Based on Tables III and IV the ratio of the bound to continuum state decay rates as a function of  $Q_m$  is shown in Fig. 8. It can be clearly observed from the figure that for the transitions having high  $Q_m$  values,  $\lambda_c$  dominates, whereas in

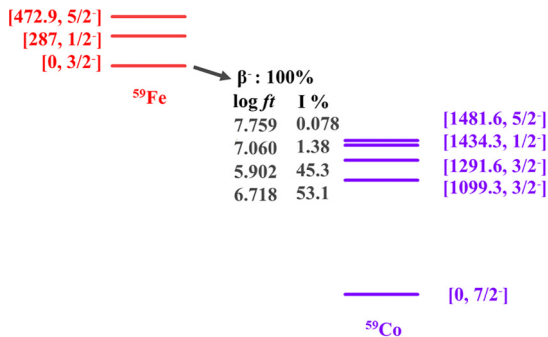


FIG. 6.  $\beta^-$  decay scheme for  $^{59}\text{Fe}$  in terrestrial laboratory. In the brackets, nuclear excitation energy ( $E_X$ ) in keV and  $J^\pi$  (spin-parity) are shown.  $I$  is the  $\beta^-$  branching.

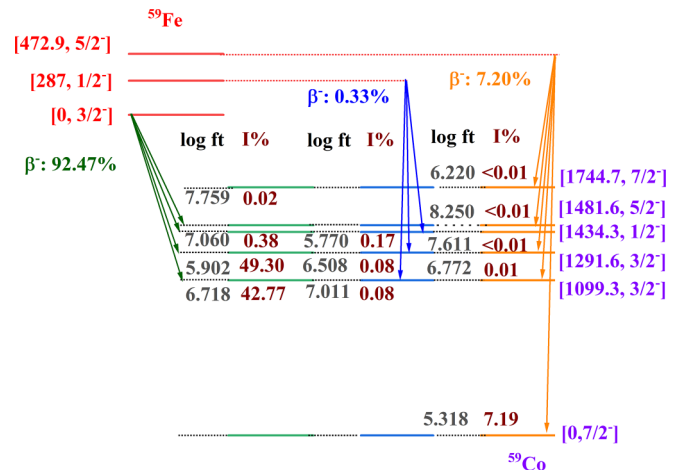


FIG. 7.  $\beta^-$  decay scheme for  $^{59}\text{Fe}$  in stellar scenario,  $T = 5 \times 10^8 \text{ K}$  and  $n_e = 10^{26} \text{ cm}^{-3}$ . In the brackets nuclear excitation energy ( $E_X$ ) in keV and  $J^\pi$  (spin-parity) are shown.  $I$  is the  $\beta^-$  branching.

TABLE V. Calculated bare atom  $\beta^-$  decay rate [ $\lambda_k$ , where  $\lambda_k = (\lambda_b + \lambda_c) \times n_{ik}$ ; in  $s^{-1}$ ] and branching ( $I_k$ ) from each parent level to daughter level  $m$  with branching ( $I_m$ ) for various density-temperature combinations. Column 2, spin-parity of parent energy levels; columns 7 and 12, spin-parity of daughter energy levels. Temperature ( $T$ ) is given in columns 3, 8, and 13, where  $T_1 = 1 \times 10^8$  K,  $T_3 = 3 \times 10^8$  K, and  $T_5 = 5 \times 10^8$  K, respectively. Column 4, equilibrium population of the  $k$ th nuclear state of the  $i$ th nucleus ( $n_{ik}$ ) at different temperatures. Columns 5 and 10, total  $\beta^-$  branching ( $I_k$ ) from each parent level at different density-temperature combinations. Columns 6 and 11, stellar  $\beta^-$  decay rate ( $\lambda_k$ ) of bare atom  $i$  from its  $k$ th nuclear level. Columns 9 and 14,  $\beta^-$  branching ( $I_m$ ) to each daughter level  $m$ .

Decay	$J_p^\pi$	$T$	$n_{ik}$	$n_e = 1 \times 10^{26} \text{ cm}^{-3}$						$n_e = 1 \times 10^{27} \text{ cm}^{-3}$					
				$I_k(\%)$	$\lambda_k$	$J_d^\pi$	$T$	$I_m(\%)$	$I_k(\%)$	$\lambda_k$	$J_d^\pi$	$T$	$I_m(\%)$		
$^{59}\text{Fe} \rightarrow ^{59}\text{Co}$	$3/2_1^-$	$T_1$	$1.00 \times 10^0$	100.00	$2.13 \times 10^{-7}$	$3/2_1^-$	$T_1$	46.29	100.00	$2.08 \times 10^{-7}$	$3/2_1^-$	$T_1$	46.62		
		$T_3$	$1.00 \times 10^0$	100.00	$2.14 \times 10^{-7}$		$T_3$	46.26	100.00	$2.10 \times 10^{-7}$		$T_3$	46.48		
		$T_5$	$9.99 \times 10^{-1}$	92.47	$2.14 \times 10^{-7}$		$T_5$	42.77	92.40	$2.11 \times 10^{-7}$		$T_5$	42.90		
		$T_1$					$3/2_2^-$	$T_1$	53.27				$3/2_2^-$	$T_1$	52.96
		$T_3$						$T_3$	53.30					$T_3$	53.09
		$T_5$						$T_5$	49.30					$T_5$	49.09
	$T_1$				$1/2_1^-$	$T_1$	0.41			$1/2_1^-$	$T_1$	0.40			
	$T_3$					$T_3$	0.41				$T_3$	0.41			
	$T_5$					$T_5$	0.38				$T_5$	0.38			
	$T_1$				$5/2_1^-$	$T_1$	0.02			$5/2_1^-$	$T_1$	0.02			
	$T_3$					$T_3$	0.02				$T_3$	0.02			
	$T_5$					$T_5$	0.02				$T_5$	0.02			
	$T_1$				$1/2_1^-$	$T_1$	0.00			$1/2_1^-$	$T_1$	0.00			
	$T_3$					$T_3$	0.00				$T_3$	0.00			
	$T_5$	$6.38 \times 10^{-4}$	0.33	$7.55 \times 10^{-10}$		$T_5$	0.08	0.33	$7.48 \times 10^{-10}$		$T_5$	0.08			
	$T_1$				$3/2_2^-$	$T_1$	0.00			$3/2_2^-$	$T_1$	0.00			
	$T_3$					$T_3$	0.00				$T_3$	0.00			
	$T_5$					$T_5$	0.08				$T_5$	0.08			
	$T_1$				$1/2_1^-$	$T_1$	0.00			$1/2_1^-$	$T_1$	0.00			
	$T_3$					$T_3$	0.00				$T_3$	0.00			
	$T_5$					$T_5$	0.17				$T_5$	0.17			
	$T_1$				$5/2_1^-$	$T_1$	0.00			$5/2_1^-$	$T_1$	0.00			
	$T_3$					$T_3$	0.00				$T_3$	0.00			
	$T_5$	$2.55 \times 10^{-5}$	7.20	$1.66 \times 10^{-8}$		$T_5$	7.19	7.29	$1.66 \times 10^{-8}$		$T_5$	7.27			
$T_1$				$3/2_1^-$	$T_1$	0.00			$3/2_1^-$	$T_1$	0.00				
$T_3$					$T_3$	0.00				$T_3$	0.00				
$T_5$					$T_5$	0.01				$T_5$	0.01				
$^{60}\text{Co} \rightarrow ^{60}\text{Ni}$	$5_1^+$	$T_1$	$1.00 \times 10^0$	97.18	$4.54 \times 10^{-9}$	$4_1^+$	$T_1$	97.18	99.68	$4.44 \times 10^{-9}$	$4_1^+$	$T_1$	99.68		
		$T_3$	$9.56 \times 10^{-1}$	26.56	$4.35 \times 10^{-9}$		$T_3$	26.56	26.40	$4.29 \times 10^{-9}$		$T_3$	26.40		
		$T_5$	$8.95 \times 10^{-1}$	11.91	$4.07 \times 10^{-9}$		$T_5$	11.91	11.86	$4.03 \times 10^{-9}$		$T_5$	11.86		
	$2_1^+$	$T_1$	$4.87 \times 10^{-4}$	2.82	$1.32 \times 10^{-10}$	$2_1^+$	$T_1$	0.31	0.32	$1.43 \times 10^{-11}$	$2_1^+$	$T_1$	0.03		
		$T_3$	$4.45 \times 10^{-2}$	73.43	$1.20 \times 10^{-8}$		$T_3$	7.97	73.59	$1.20 \times 10^{-8}$		$T_3$	8.02		
		$T_5$	$1.04 \times 10^{-1}$	81.96	$2.80 \times 10^{-8}$		$T_5$	8.90	82.07	$2.79 \times 10^{-8}$		$T_5$	8.93		
	$2_2^+$	$T_1$				$2_2^+$	$T_1$	2.51			$2_2^+$	$T_1$	0.29		
		$T_3$					$T_3$	65.45				$T_3$	65.57		
		$T_5$					$T_5$	73.06				$T_5$	73.14		
	$4_1^+$	$T_1$	$0.00 \times 10^0$	0.00	$0.00 \times 10^0$	$4_1^+$	$T_1$	0.00	0.00	$0.00 \times 10^0$	$4_1^+$	$T_1$	0.00		
		$T_3$	$1.72 \times 10^{-5}$	0.01	$1.63 \times 10^{-12}$		$T_3$	0.01	0.01	$1.62 \times 10^{-12}$		$T_3$	0.01		
		$T_5$	$1.17 \times 10^{-3}$	0.33	$1.12 \times 10^{-10}$		$T_5$	0.32	0.33	$1.11 \times 10^{-10}$		$T_5$	0.32		
	$3_1^+$	$T_1$				$3_1^+$	$T_1$	0.00			$3_1^+$	$T_1$	0.00		
		$T_3$					$T_3$	0.00				$T_3$	0.00		
		$T_5$					$T_5$	0.01				$T_5$	0.01		

TABLE V. (Continued.)

Decay	$J_p^\pi$	$T$	$n_{ik}$	$n_e = 1 \times 10^{26} \text{ cm}^{-3}$					$n_e = 1 \times 10^{27} \text{ cm}^{-3}$																	
				$I_k(\%)$	$\lambda_k$	$J_d^\pi$	$T$	$I_m(\%)$	$I_k(\%)$	$\lambda_k$	$J_d^\pi$	$T$	$I_m(\%)$													
$^{61}\text{Co} \rightarrow ^{61}\text{Ni}$	$3_1^+$	$T_1$	$0.00 \times 10^0$	0.00	$0.00 \times 10^0$	$2_1^+$	$T_1$	0.00	0.00	$0.00 \times 10^0$	$2_1^+$	$T_1$	0.00													
		$T_3$	$0.00 \times 10^0$	0.00	$0.00 \times 10^0$		$T_3$	0.00	0.00	$0.00 \times 10^0$		$T_3$	0.00													
		$T_5$	$7.03 \times 10^{-4}$	5.73	$1.96 \times 10^{-9}$		$T_5$	0.38	5.74	$1.95 \times 10^{-9}$		$T_5$	0.38													
															$2_2^+$	$T_1$	0.00	$2_2^+$	$T_1$	0.00						
																$T_3$	0.00		$T_3$	0.00						
	$T_5$	4.92	$T_5$	4.92																						
															$4_1^+$	$T_1$	0.00	$4_1^+$	$T_1$	0.00						
																$T_3$	0.00		$T_3$	0.00						
	$T_5$	0.43	$T_5$	0.43																						
$3_1^+$															$T_1$	0.00	$3_1^+$	$T_1$	0.00							
															$T_3$	0.00		$T_3$	0.00							
	$T_5$	0.01	$T_5$	0.01																						
	$7/2_1^-$	$T_1$	$1.00 \times 10^0$	100.00	$1.02 \times 10^{-4}$	$5/2_1^-$	$T_1$	98.74	100.00	$1.03 \times 10^{-4}$	$5/2_1^-$	$T_1$	98.77													
		$T_3$	$1.00 \times 10^0$	100.00	$1.02 \times 10^{-4}$		$T_3$	98.74	100.00	$1.03 \times 10^{-4}$		$T_3$	98.76													
		$T_5$	$1.00 \times 10^0$	100.00	$1.02 \times 10^{-4}$		$T_5$	98.74	100.00	$1.03 \times 10^{-4}$		$T_5$	98.76													
														$5/2_2^-$	$T_1$	0.37	$5/2_2^-$	$T_1$	0.37							
															$T_3$	0.37		$T_3$	0.37							
$T_5$	0.37	$T_5$	0.37																							
														$7/2_1^-$	$T_1$	0.54	$7/2_1^-$	$T_1$	0.53							
															$T_3$	0.54		$T_3$	0.54							
$T_5$	0.54	$T_5$	0.54																							
														$7/2_2^-$	$T_1$	0.15	$7/2_2^-$	$T_1$	0.15							
															$T_3$	0.15		$T_3$	0.15							
$T_5$	0.15	$T_5$	0.15																							
														$5/2_3^-$	$T_1$	0.19	$5/2_3^-$	$T_1$	0.18							
															$T_3$	0.19		$T_3$	0.18							
$T_5$	0.19	$T_5$	0.19																							
$^{63}\text{Ni} \rightarrow ^{63}\text{Cu}$	$1/2_1^-$	$T_1$	$1.00 \times 10^0$	99.60	$1.01 \times 10^{-9}$	$3/2_1^-$	$T_1$	99.60	99.59	$9.21 \times 10^{-10}$	$3/2_1^-$	$T_1$	99.59													
		$T_3$	$9.03 \times 10^{-1}$	17.76	$9.18 \times 10^{-10}$		$T_3$	17.76	17.37	$8.64 \times 10^{-10}$		$T_3$	17.37													
		$T_5$	$6.90 \times 10^{-1}$	3.60	$7.04 \times 10^{-10}$		$T_5$	3.60	3.51	$6.75 \times 10^{-10}$		$T_5$	3.51													
														$5/2_1^-$	$T_1$	$1.20 \times 10^{-4}$	0.40	$4.02 \times 10^{-12}$	$3/2_1^-$	$T_1$	0.40	0.41	$3.82 \times 10^{-12}$	$3/2_1^-$	$T_1$	0.41
															$T_3$	$9.27 \times 10^{-2}$	60.23	$3.11 \times 10^{-9}$		$T_3$	60.23	60.36	$3.00 \times 10^{-9}$		$T_3$	60.36
$T_5$	$2.73 \times 10^{-1}$	46.95	$9.19 \times 10^{-9}$	$T_5$	46.95	46.81	$8.92 \times 10^{-9}$	$T_5$	46.81																	
														$3/2_1^-$	$T_1$	$0.00 \times 10^0$	0.00	$0.00 \times 10^0$	$3/2_1^-$	$T_1$	0.00	0.00	$0.00 \times 10^0$	$3/2_1^-$	$T_1$	0.00
															$T_3$	$4.38 \times 10^{-3}$	22.02	$1.14 \times 10^{-9}$		$T_3$	22.02	22.27	$1.11 \times 10^{-9}$		$T_3$	22.27
$T_5$	$3.72 \times 10^{-2}$	49.45	$9.68 \times 10^{-9}$	$T_5$	49.45	49.67	$9.46 \times 10^{-9}$	$T_5$	49.67																	
$^{65}\text{Ni} \rightarrow ^{65}\text{Cu}$	$5/2_1^-$	$T_1$	$1.00 \times 10^0$	98.44	$7.29 \times 10^{-5}$	$3/2_1^-$	$T_1$	61.29	98.43	$7.24 \times 10^{-5}$	$3/2_1^-$	$T_1$	61.50													
		$T_3$	$9.72 \times 10^{-1}$	31.79	$7.10 \times 10^{-5}$		$T_3$	19.79	31.74	$7.06 \times 10^{-5}$		$T_3$	19.80													
		$T_5$	$9.29 \times 10^{-1}$	14.85	$6.69 \times 10^{-5}$		$T_5$	9.25	14.83	$6.75 \times 10^{-5}$		$T_5$	9.25													
														$5/2_1^-$	$T_1$	4.99	$5/2_1^-$	$T_1$	4.99							
															$T_3$	1.61		$T_3$	1.61							
$T_5$	0.75	$T_5$	0.75																							
														$7/2_1^-$	$T_1$	29.27	$7/2_1^-$	$T_1$	29.09							
															$T_3$	9.46		$T_3$	9.40							
$T_5$	4.41	$T_5$	4.40																							
														$5/2_2^-$	$T_1$	2.65	$5/2_2^-$	$T_1$	2.62							
															$T_3$	0.86		$T_3$	0.85							
$T_5$	0.40	$T_5$	0.40																							
														$3/2_2^-$	$T_1$	0.22	$3/2_2^-$	$T_1$	0.22							
															$T_3$	0.07		$T_3$	0.07							
$T_5$	0.03	$T_5$	0.03																							



TABLE V. (Continued.)

Decay	$J_p^\pi$	$T$	$n_{ik}$	$n_e = 1 \times 10^{26} \text{ cm}^{-3}$					$n_e = 1 \times 10^{27} \text{ cm}^{-3}$				
				$I_k(\%)$	$\lambda_k$	$J_d^\pi$	$T$	$I_m(\%)$	$I_k(\%)$	$\lambda_k$	$J_d^\pi$	$T$	$I_m(\%)$
						$7/2_2^-$	$T_1$	0.02			$7/2_2^-$	$T_1$	0.01
							$T_3$	0.01				$T_3$	0.00
							$T_5$	0.00				$T_5$	0.00
	$1/2_1^-$	$T_1$	$2.12 \times 10^{-4}$	1.56	$1.16 \times 10^{-6}$	$3/2_1^-$	$T_1$	1.56	1.57	$1.15 \times 10^{-6}$	$3/2_1^-$	$T_1$	1.56
		$T_3$	$2.79 \times 10^{-2}$	68.21	$1.52 \times 10^{-4}$		$T_3$	67.90	68.26	$1.52 \times 10^{-4}$		$T_3$	67.95
		$T_5$	$7.10 \times 10^{-2}$	85.06	$3.83 \times 10^{-4}$		$T_5$	84.68	85.08	$3.87 \times 10^{-4}$		$T_5$	84.69
						$1/2_1^-$	$T_1$	0.01			$1/2_1^-$	$T_1$	0.01
							$T_3$	0.30				$T_3$	0.30
							$T_5$	0.38				$T_5$	0.38
						$3/2_2^-$	$T_1$	0.00			$3/2_2^-$	$T_1$	0.00
							$T_3$	0.00				$T_3$	0.00
							$T_5$	0.01				$T_5$	0.01
$^{66}\text{Ni} \rightarrow ^{66}\text{Cu}$	$0_1^+$	$T_1$	$1.00 \times 10^0$	100.00	$3.91 \times 10^{-6}$	$0_1^+$	$T_1$	100.00	100.00	$3.78 \times 10^{-6}$	$0_1^+$	$T_1$	100.00
		$T_3$	$1.00 \times 10^0$	100.00	$3.92 \times 10^{-6}$		$T_3$	100.00	100.00	$3.83 \times 10^{-6}$		$T_3$	100.00
		$T_5$	$1.00 \times 10^0$	100.00	$3.93 \times 10^{-6}$		$T_5$	100.00	100.00	$3.85 \times 10^{-6}$		$T_5$	100.00
$^{64}\text{Cu} \rightarrow ^{64}\text{Zn}$	$1_1^+$	$T_1$	$1.00 \times 10^0$	100.00	$5.42 \times 10^{-6}$	$0_1^+$	$T_1$	100.00	100.00	$5.34 \times 10^{-6}$	$0_1^+$	$T_1$	100.00
		$T_3$	$1.00 \times 10^0$	100.00	$5.43 \times 10^{-6}$		$T_3$	100.00	100.00	$5.37 \times 10^{-6}$		$T_3$	100.00
		$T_5$	$1.00 \times 10^0$	100.00	$5.43 \times 10^{-6}$		$T_5$	100.00	100.00	$5.38 \times 10^{-6}$		$T_5$	100.00
$^{66}\text{Cu} \rightarrow ^{66}\text{Zn}$	$1_1^+$	$T_1$	$1.00 \times 10^0$	100.00	$1.55 \times 10^{-3}$	$0_1^+$	$T_1$	77.03	100.00	$1.55 \times 10^{-3}$	$0_1^+$	$T_1$	77.07
		$T_3$	$9.99 \times 10^{-1}$	99.98	$1.55 \times 10^{-3}$		$T_3$	77.01	99.98	$1.55 \times 10^{-3}$		$T_3$	77.04
		$T_5$	$9.74 \times 10^{-1}$	99.60	$1.51 \times 10^{-3}$		$T_5$	76.72	99.59	$1.51 \times 10^{-3}$		$T_5$	76.74
						$2_1^+$	$T_1$	22.82			$2_1^+$	$T_1$	22.78
							$T_3$	22.81				$T_3$	22.79
							$T_5$	22.73				$T_5$	22.71
						$2_2^+$	$T_1$	0.15			$2_2^+$	$T_1$	0.15
							$T_3$	0.15				$T_3$	0.15
							$T_5$	0.15				$T_5$	0.15
$^{67}\text{Cu} \rightarrow ^{67}\text{Zn}$	$3/2_1^-$	$T_1$	$1.00 \times 10^0$	100.00	$2.98 \times 10^{-6}$	$5/2_1^-$	$T_1$	39.50	100.00	$2.94 \times 10^{-6}$	$5/2_1^-$	$T_1$	39.64
		$T_3$	$1.00 \times 10^0$	100.00	$2.99 \times 10^{-6}$		$T_3$	39.48	100.00	$2.96 \times 10^{-6}$		$T_3$	39.57
		$T_5$	$1.00 \times 10^0$	100.00	$2.99 \times 10^{-6}$		$T_5$	39.48	100.00	$2.97 \times 10^{-6}$		$T_5$	39.54
						$1/2_1^-$	$T_1$	21.32			$1/2_1^-$	$T_1$	21.34
							$T_3$	21.31				$T_3$	21.33
							$T_5$	21.31				$T_5$	21.32
						$3/2_1^-$	$T_1$	36.70			$3/2_1^-$	$T_1$	36.60
							$T_3$	36.72				$T_3$	36.65
							$T_5$	36.72				$T_5$	36.67
						$3/2_2^-$	$T_1$	2.48			$3/2_2^-$	$T_1$	2.42
							$T_3$	2.49				$T_3$	2.45
							$T_5$	2.49				$T_5$	2.46
$^{69}\text{Zn} \rightarrow ^{69}\text{Ga}$	$1/2_1^-$	$T_1$	$1.00 \times 10^0$	100.00	$2.19 \times 10^{-4}$	$3/2_1^-$	$T_1$	99.98	100.00	$2.17 \times 10^{-4}$	$3/2_1^-$	$T_1$	99.98
		$T_3$	$1.00 \times 10^0$	100.00	$2.19 \times 10^{-4}$		$T_3$	99.98	100.00	$2.18 \times 10^{-4}$		$T_3$	99.98
		$T_5$	$1.00 \times 10^0$	100.00	$2.19 \times 10^{-4}$		$T_5$	99.98	100.00	$2.18 \times 10^{-4}$		$T_5$	99.98
						$1/2_1^-$	$T_1$	0.01			$1/2_1^-$	$T_1$	0.01
							$T_3$	0.01				$T_3$	0.01
							$T_5$	0.01				$T_5$	0.01
$^{72}\text{Zn} \rightarrow ^{72}\text{Ga}$	$0_1^+$	$T_1$	$1.00 \times 10^0$	100.00	$6.81 \times 10^{-6}$	$0_1^+$	$T_1$	0.14	100.00	$6.59 \times 10^{-6}$	$0_1^+$	$T_1$	0.14
		$T_3$	$1.00 \times 10^0$	100.00	$6.83 \times 10^{-6}$		$T_3$	0.14	100.00	$6.68 \times 10^{-6}$		$T_3$	0.14
		$T_5$	$1.00 \times 10^0$	100.00	$6.84 \times 10^{-6}$		$T_5$	0.14	100.00	$6.71 \times 10^{-6}$		$T_5$	0.14
						$1,2$	$T_1$	37.85			$1,2$	$T_1$	37.97

TABLE V. (Continued.)

Decay	$J_p^\pi$	$T$	$n_{ik}$	$n_e = 1 \times 10^{26} \text{ cm}^{-3}$					$n_e = 1 \times 10^{27} \text{ cm}^{-3}$						
				$I_k(\%)$	$\lambda_k$	$J_d^\pi$	$T$	$I_m(\%)$	$I_k(\%)$	$\lambda_k$	$J_d^\pi$	$T$	$I_m(\%)$		
$^{70}\text{Ga} \rightarrow ^{70}\text{Ge}$	$1_1^+$	$T_1$	$1.00 \times 10^0$	100.00	$5.49 \times 10^{-4}$	$0_1^+$	$T_3$	37.84	100.00	$5.46 \times 10^{-4}$	$0_1^+$	$T_3$	37.92		
							$T_5$	37.83				$T_5$	37.90		
							$T_3$	39.30				$T_3$	39.31		
							$T_5$	39.30				$T_5$	39.31		
							$T_3$	22.71				$T_3$	22.58		
							$T_5$	22.72				$T_5$	22.64		
							$T_3$	22.73				$T_3$	22.66		
							$T_5$	22.73				$T_5$	22.66		
							$T_3$	96.85				$T_3$	96.88		
							$T_5$	96.85				$T_5$	96.87		
							$T_3$	96.84				$T_3$	96.87		
							$T_5$	96.84				$T_5$	96.87		
$^{75}\text{Ge} \rightarrow ^{75}\text{As}$	$1/2_1^-$	$T_1$	$1.00 \times 10^0$	100.00	$1.49 \times 10^{-4}$	$3/2_1^-$	$T_1$	84.23	100.00	$1.48 \times 10^{-4}$	$3/2_1^-$	$T_1$	84.29		
							$T_3$	84.20				$T_3$	84.24		
							$T_5$	83.57				$T_5$	83.60		
							$T_1$	2.75				$T_1$	2.73		
							$T_3$	2.76				$T_3$	2.74		
							$T_5$	2.76				$T_5$	2.74		
							$T_1$	0.40				$T_1$	0.39		
							$T_3$	0.40				$T_3$	0.39		
							$T_5$	0.40				$T_5$	0.39		
							$T_1$	$9.78 \times 10^{-1}$				$T_1$	84.23	$T_1$	84.29
							$T_3$	$9.78 \times 10^{-1}$				$T_3$	84.20	$T_3$	84.24
							$T_5$	$8.03 \times 10^{-1}$				$T_5$	83.57	$T_5$	83.60
							$T_1$	0.44				$T_1$	0.44	$T_1$	0.44
							$T_3$	0.44				$T_3$	0.44	$T_3$	0.44
							$T_5$	0.44				$T_5$	0.44	$T_5$	0.44
							$T_1$	11.14				$T_1$	11.12	$T_1$	11.12
							$T_3$	11.13				$T_3$	11.12	$T_3$	11.12
							$T_5$	11.05				$T_5$	11.04	$T_5$	11.04
							$T_1$	0.16				$T_1$	0.16	$T_1$	0.16
							$T_3$	0.16				$T_3$	0.16	$T_3$	0.16
							$T_5$	16.00				$T_5$	0.16	$T_5$	0.16
							$T_1$	3.53				$T_1$	3.50	$T_1$	3.50
							$T_3$	3.53				$T_3$	3.51	$T_3$	3.51
							$T_5$	3.50				$T_5$	3.48	$T_5$	3.48
$T_1$	0.50	$T_1$	0.49	$T_1$	0.49										
$T_3$	0.50	$T_3$	0.49	$T_3$	0.49										
$T_5$	0.49	$T_5$	0.49	$T_5$	0.49										
$T_1$	0.01	$T_1$	0.01	$T_1$	0.01										
$T_3$	0.01	$T_3$	0.01	$T_3$	0.01										
$T_5$	0.01	$T_5$	0.01	$T_5$	0.01										
$^{75}\text{Ge} \rightarrow ^{75}\text{As}$	$7/2_1^+$	$T_1$	$0.00 \times 10^0$	0.00	$0.00 \times 10^0$	$5/2_1^+$	$T_1$	0.00	0.00	$0.00 \times 10^0$	$5/2_1^+$	$T_1$	0.00		
			$1.76 \times 10^{-2}$	0.02	$1.97 \times 10^{-8}$	$T_3$	0.01	0.01	$1.96 \times 10^{-8}$	$T_3$	0.01				
			$1.25 \times 10^{-1}$	0.12	$1.41 \times 10^{-7}$	$T_5$	0.04	0.12	$1.40 \times 10^{-7}$	$T_5$	0.04				
			$T_1$	0.00	$T_1$	0.00	$T_1$	0.00							
			$T_3$	0.01	$T_3$	0.01	$T_3$	0.01							
			$T_5$	0.06	$T_5$	0.06	$T_5$	0.06							
$^{75}\text{Ge} \rightarrow ^{75}\text{As}$	$3/2_1^-$	$T_1$	$0.00 \times 10^0$	0.00	$0.00 \times 10^0$	$3/2_1^-$	$T_1$	0.00	0.00	$0.00 \times 10^0$	$3/2_1^-$	$T_1$	0.00		
			$1.09 \times 10^{-4}$	0.01	$1.37 \times 10^{-8}$	$T_3$	0.01	0.01	$1.36 \times 10^{-8}$	$T_3$	0.01				
			$4.50 \times 10^{-3}$	0.47	$5.67 \times 10^{-7}$	$T_5$	0.28	0.47	$5.64 \times 10^{-7}$	$T_5$	0.28				
			$T_1$	0.00	$T_1$	0.00	$T_1$	0.00							
			$T_3$	0.00	$T_3$	0.00	$T_3$	0.00							
			$T_5$	0.00	$T_5$	0.00	$T_5$	0.00							

TABLE V. (Continued.)

Decay	$J_p^\pi$	$T$	$n_{ik}$	$n_e = 1 \times 10^{26} \text{ cm}^{-3}$					$n_e = 1 \times 10^{27} \text{ cm}^{-3}$				
				$I_k(\%)$	$\lambda_k$	$J_d^\pi$	$T$	$I_m(\%)$	$I_k(\%)$	$\lambda_k$	$J_d^\pi$	$T$	$I_m(\%)$
$^{78}\text{Ge} \rightarrow ^{78}\text{As}$	$0_1^+$	$T_1$	$1.00 \times 10^0$	100.00	$1.43 \times 10^{-4}$	$1_1^+$	$T_1$	39.54	100.00	$1.41 \times 10^{-4}$	$1_1^+$	$T_1$	39.71
		$T_3$	$1.00 \times 10^0$	100.00	$1.44 \times 10^{-4}$	$T_3$	39.52	100.00	$1.42 \times 10^{-4}$	$T_3$	39.64		
		$T_5$	$1.00 \times 10^0$	100.00	$1.44 \times 10^{-4}$	$T_5$	39.51	100.00	$1.42 \times 10^{-4}$	$T_5$	39.62		
		$T_5$				$T_5$	0.13			$T_5$	0.13		
		$T_1$				$T_1$	0.00			$T_1$	0.00		
		$T_3$				$T_3$	0.00			$T_3$	0.00		
	$1_2^+$	$T_1$	$1.00 \times 10^0$	100.00	$5.86 \times 10^{-4}$	$3/2_1^-$	$T_1$	98.74	100.00	$5.95 \times 10^{-4}$	$3/2_1^-$	$T_1$	98.74
		$T_3$	$9.31 \times 10^{-1}$	99.99	$5.46 \times 10^{-4}$	$T_3$	98.72	99.99	$5.55 \times 10^{-4}$	$T_3$	98.73		
		$T_5$	$7.29 \times 10^{-1}$	99.90	$4.28 \times 10^{-4}$	$T_5$	98.65	99.92	$4.35 \times 10^{-4}$	$T_5$	98.66		
		$T_1$				$T_1$	0.02			$T_1$	0.02		
		$T_3$				$T_3$	0.02			$T_3$	0.02		
		$T_5$				$T_5$	0.02			$T_5$	0.02		
$^{81}\text{Se} \rightarrow ^{81}\text{Br}$	$1/2_1^-$	$T_1$	$1.00 \times 10^0$	100.00	$5.86 \times 10^{-4}$	$3/2_2^-$	$T_1$	0.10	100.00	$5.95 \times 10^{-4}$	$3/2_2^-$	$T_1$	0.10
		$T_3$	$9.31 \times 10^{-1}$	99.99	$5.46 \times 10^{-4}$	$T_3$	0.10	99.99	$5.55 \times 10^{-4}$	$T_3$	0.10		
		$T_5$	$7.29 \times 10^{-1}$	99.90	$4.28 \times 10^{-4}$	$T_5$	0.10	99.92	$4.35 \times 10^{-4}$	$T_5$	0.10		
	$3/2_2^-$	$T_1$	$1.00 \times 10^0$	100.00	$5.86 \times 10^{-4}$	$(3/2^-)_3$	$T_1$	0.18	100.00	$5.95 \times 10^{-4}$	$(3/2^-)_3$	$T_1$	0.18
		$T_3$	$9.31 \times 10^{-1}$	99.99	$5.46 \times 10^{-4}$	$T_3$	0.18	99.99	$5.55 \times 10^{-4}$	$T_3$	0.18		
		$T_5$	$7.29 \times 10^{-1}$	99.90	$4.28 \times 10^{-4}$	$T_5$	0.18	99.92	$4.35 \times 10^{-4}$	$T_5$	0.18		
	$3/2_4^-$	$T_1$	$1.00 \times 10^0$	100.00	$5.86 \times 10^{-4}$	$3/2_4^-$	$T_1$	0.92	100.00	$5.95 \times 10^{-4}$	$3/2_4^-$	$T_1$	0.91
		$T_3$	$9.31 \times 10^{-1}$	99.99	$5.46 \times 10^{-4}$	$T_3$	0.92	99.99	$5.55 \times 10^{-4}$	$T_3$	0.92		
		$T_5$	$7.29 \times 10^{-1}$	99.90	$4.28 \times 10^{-4}$	$T_5$	0.92	99.92	$4.35 \times 10^{-4}$	$T_5$	0.92		
	$1/2_2^-$	$T_1$	$1.00 \times 10^0$	100.00	$5.86 \times 10^{-4}$	$1/2_2^-$	$T_1$	0.03	100.00	$5.95 \times 10^{-4}$	$1/2_2^-$	$T_1$	0.03
		$T_3$	$9.31 \times 10^{-1}$	99.99	$5.46 \times 10^{-4}$	$T_3$	0.03	99.99	$5.55 \times 10^{-4}$	$T_3$	0.03		
		$T_5$	$7.29 \times 10^{-1}$	99.90	$4.28 \times 10^{-4}$	$T_5$	0.03	99.92	$4.35 \times 10^{-4}$	$T_5$	0.03		

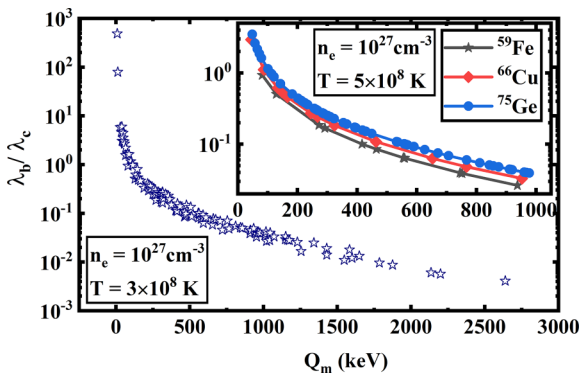


FIG. 8. Variation of the ratio of bound state ( $\lambda_b$ ) to continuum state ( $\lambda_c$ ) decay rates with  $Q_m$  for a stellar density; temperature combination as shown. Spread in the ratio is due to a dependence on  $Z$ , and  $A$  of the daughter nuclei is shown in the inset. See text for details.

the case of transitions having comparatively lower  $Q_m$  values,  $\lambda_b$  starts to compete with  $\lambda_c$ . From Fig. 8, it can be said that for these nuclei, the transitions having  $Q_m$  below  $\approx 100$  keV, the bound state decay rates dominate over continuum state decay rates. The ratio falls from 1 to  $\approx 10^{-3}$  for  $100 < Q_m < 2800$  keV. Moreover, it is also to be noted that the  $\lambda_b/\lambda_c$  ratio is dependent on the atomic number ( $Z$ ) and mass number ( $A$ ) of the daughter nucleus. As the  $Z$  and  $A$  values increase, the ratio increases slightly, causing a spread in the curve as shown in Fig. 8. In the inset of Fig. 8, we illustrate the  $Z$  and  $A$  dependence for a higher temperature to accommodate more transitions. This dependence is actually coming from the phase space factor of the continuum decay and through the large component of the Dirac radial wave function in the case of bound state decay. This points to the fact that bound state decay is more important for transitions with low  $Q$  values. For the set of nuclei, the bound state decay contribution to total  $\beta^-$  decay ranges from about 1% to 62%, as shown in Tables VI and VII. For nuclei having decays from a large

TABLE VI. Variation of bound state  $\beta^-$  decay contribution (in %) for individual transition and to the total decay, with temperature at a free electron density. Columns 5 and 7, bound state  $\beta^-$  decay contribution in individual transition. Columns 6 and 8, contribution to total decay rate from bound state decay. See text for more details.

				$n_e = 1 \times 10^{27} \text{ cm}^{-3}$			
				$T = 1 \times 10^8 \text{ K}$		$T = 5 \times 10^8 \text{ K}$	
Transition details				Bound state decay contribution (%) in individual transition	Bound state decay contribution (%) in total $\beta^-$ decay	Bound state decay contribution (%) in individual transition	Bound state decay contribution (%) in total $\beta^-$ decay
Decay	$J_p^\pi$	$J_d^\pi$	$Q_n$ (keV)				
$^{59}\text{Fe} \rightarrow ^{59}\text{Co}$	$3/2_1^-$	$3/2_1^-$	465.7	7.86	12.18	7.81	11.22
		$3/2_2^-$	273.4	15.80		15.62	
		$1/2_1^-$	130.7	34.28		33.56	
		$5/2_1^-$	83.4	49.47		48.14	
	$1/2_1^-$	$3/2_1^-$	752.723			3.74	
		$3/2_2^-$	560.423			5.96	
		$1/2_1^-$	417.723			9.09	
	$5/2_1^-$	$7/2_1^-$	2037.87			0.56	
		$3/2_1^-$	938.57			2.56	
		$3/2_2^-$	746.27			3.79	
$5/2_1^-$		556.27			6.03		
$7/2_2^-$		293.18			14.37		
$^{60}\text{Co} \rightarrow ^{60}\text{Ni}$	$5_1^+$	$4_1^+$	317.047	14.15	12.53	14.02	1.59
	$2_1^+$	$2_1^+$	1549.19	1.08		1.08	
		$2_2^+$	723.09	4.36		4.34	
	$4_1^+$	$4_1^+$	594.247			5.90	
		$3_1^+$	473.94			8.23	
	$3_1^+$	$2_1^+$	1778.7			0.81	
		$2_2^+$	952.6			2.72	
		$4_1^+$	605.447			5.74	
		$3_1^+$	485.14			7.96	
		$5_2^+$	752.757			4.06	
$5_2^+$	$4_1^+$	138.64			33.69		
	$4_2^+$						
$^{61}\text{Co} \rightarrow ^{61}\text{Ni}$	$7/2_1^-$	$5/2_1^-$	1256.4	1.64	1.78	1.63	1.77
		$5/2_2^-$	415.19	9.96		9.89	
		$7/2_1^-$	1320.8	10.26		10.18	
		$7/2_2^-$	308.56	14.63		14.49	
		$5/2_3^-$	191.46	25.12		24.74	
$^{63}\text{Ni} \rightarrow ^{63}\text{Cu}$	$1/2_1^-$	$3/2_1^-$	66.945	62.03	61.91	60.38	28.43
	$5/2_1^-$	$3/2_1^-$	154.095	32.94		32.34	
	$3/2_1^-$	$3/2_1^-$	222.495	22.78		22.48	
$^{65}\text{Ni} \rightarrow ^{65}\text{Cu}$	$5/2_1^-$	$3/2_1^-$	2137.9	0.60	2.35	0.60	0.83
		$5/2_1^-$	1022.3	2.61		2.60	
		$7/2_1^-$	656.1	5.50		5.47	
		$5/2_2^-$	514.5	7.93		7.89	
		$3/2_2^-$	2132.9	10.78		10.70	
		$7/2_2^-$	43.56	76.84		74.86	
		$5/2_3^-$	30.5	86.82		84.95	
$1/2_1^-$	$3/2_1^-$	2201.27	0.56		0.56		
	$1/2_1^-$	1430.63	1.38		1.38		
	$3/2_2^-$	476.27	8.86		8.80		
$^{66}\text{Ni} \rightarrow ^{66}\text{Cu}$	$0_1^+$	$1_1^+$	251.9	19.86	19.86	19.63	19.63
$^{64}\text{Cu} \rightarrow ^{64}\text{Zn}$	$1_1^+$	$0_1^+$	579.6	7.15	7.15	7.12	7.12

TABLE VI. (Continued.)

Transition details				$n_e = 1 \times 10^{27} \text{ cm}^{-3}$				
				$T = 1 \times 10^8 \text{ K}$		$T = 5 \times 10^8 \text{ K}$		
				Bound state decay contribution (%) in individual transition	Bound state decay contribution (%) in total $\beta^-$ decay	Bound state decay contribution (%) in individual transition	Bound state decay contribution (%) in total $\beta^-$ decay	
Decay	$J_p^\pi$	$J_d^\pi$	$Q_n(\text{keV})$					
$^{66}\text{Cu} \rightarrow ^{66}\text{Zn}$	$1_1^+$	$0_1^+$	2640.9	0.41	0.59	0.41	0.59	
		$2_1^+$	1601.7	1.20		1.19		
		$2_2^+$	768.1	4.60		4.58		
$^{67}\text{Cu} \rightarrow ^{67}\text{Zn}$	$3/2_1^-$	$0_2^+$	269.5	19.65		19.43		
		$5/2_1^-$	561.7	7.49	10.57	7.45	10.51	
		$1/2_1^-$	468.4	9.72		9.66		
		$3/2_1^-$	377.1	13.01		12.90		
$^{69}\text{Zn} \rightarrow ^{69}\text{Ga}$	$1/2_1^-$	$3/2_2^-$	168.2	32.00		31.47		
		$3/2_1^-$	910.2	3.72	3.72	3.71	3.71	
		$1/2_1^-$	591.8	7.43		7.39		
$^{72}\text{Zn} \rightarrow ^{72}\text{Ga}$	$0_1^+$	$3/2_2^-$	38.5	83.84		82.03		
		$0_1^+$	323.6	16.77	19.83	16.61	19.62	
		$1_1^+$	314.3	17.37		17.20		
		$1_2^+$	281.7	19.74		19.53		
$^{70}\text{Ga} \rightarrow ^{70}\text{Ge}$	$1_1^+$	$1_3^+$	234.9	24.14		23.84		
		$0_1^+$	1651.7	1.31	1.52	1.31	1.52	
		$2_1^+$	612.2	7.55		7.51		
$^{75}\text{Ge} \rightarrow ^{75}\text{As}$	$1/2_1^-$	$0_2^+$	436.1	12.21		12.12		
		$3/2_1^-$	1177.2	2.71	3.13	2.70	3.12	
		$1/2_1^-$	978.594	3.78		3.76		
		$3/2_2^-$	912.542	4.26		4.25		
		$1/2_2^-$	708.46	6.44		6.41		
		$1/2_3^-$	592.2	8.46		8.42		
		$3/2_3^-$	559.52	9.19		9.14		
		$3/2_4^-$	311.8	19.66		19.47		
		$3/2_5^-$	113.9	50.66		49.64		
		$3/2_6^-$	102.7	54.47		53.33		
		$1/2_4^-$	50.2	79.38		77.67		
		$1/2_5^-$	5.2	100.00		100.00		
		$7/2_1^+$	$9/2_1^+$	1012.97			3.54	
			$5/2_1^+$	916.232			4.22	
			$5/2_2^+$	236.09			26.36	
	$5/2_3^+$	216.69			28.74			
	$9/2_2^+$	55.88			74.37			
	$5/2_4^+$	14.59			98.63			
$3/2_1^-$	$3/2_1^-$	1430.35			1.87			
	$1/2_1^-$	1231.74			2.49			
	$3/2_2^-$	1165.69			2.75			
	$5/2_1^-$	1150.81			2.82			
	$1/2_2^-$	961.61			3.88			
	$5/2_2^-$	857.94			4.71			
	$1/2_3^-$	845.35			4.83			
	$3/2_3^-$	812.67			5.15			
	$3/2_4^-$	564.95			9.01			
	$3/2_5^-$	367.05			16.03			
	$3/2_6^-$	355.85			16.65			
	$1/2_4^-$	303.35			20.09			
$1/2_5^-$	258.35			23.99				

TABLE VI. (Continued.)

				$n_e = 1 \times 10^{27} \text{ cm}^{-3}$			
				$T = 1 \times 10^8 \text{ K}$		$T = 5 \times 10^8 \text{ K}$	
Transition details				Bound state decay contribution (%) in individual transition	Bound state decay contribution (%) in total $\beta^-$ decay	Bound state decay contribution (%) in individual transition	Bound state decay contribution (%) in total $\beta^-$ decay
Decay	$J_p^\pi$	$J_d^\pi$	$Q_n(\text{keV})$				
$^{78}\text{Ge} \rightarrow ^{78}\text{As}$	$0_1^+$	$3/2_7^-$	226.85			27.45	
		$3/2_8^-$	80.95			61.83	
		$3/2_9^-$	59.55			73.32	
		$5/2_3^-$	10.15			99.75	
		$1_1^+$	677.7	6.90	10.04	6.87	9.98
$^{81}\text{Se} \rightarrow ^{81}\text{Br}$	$1/2_1^-$	$1_2^+$	661.1	7.17		7.14	
		$1_3^+$	419	13.67		13.57	
		$3/2_1^-$	1585.3	1.75	1.81	1.75	1.82
		$1/2_1^-$	1047.1	3.82		3.81	
		$3/2_2^-$	1019.26	4.01		3.99	
		$3/2_3^-$	935.4	4.64		4.63	
		$3/2_4^-$	757.01	6.57		6.55	
		$1/2_2^-$	480	12.80		12.71	
		$3/2_5^-$	318.9	21.27		21.07	
		$3/2_6^-$	49.4	82.77		81.18	
$3/2_7^-$	42.1	86.86		85.34			

number of excited levels,  $Q$  values are generally large and the contribution to the bound state decay is small. As the temperature increases at a fixed density, the contribution of the bound state decay decreases due to the following facts: (i) the drop of IPD at higher temperature, which increases the  $Q_m$  value, and (ii) the contribution of nuclear excited levels, having higher  $Q_m$  values.

From Table VII it can be seen that for a fixed  $T$ , the bound state contribution is smaller at  $n_e = 10^{27} \text{ cm}^{-3}$  for higher  $Q$ -value ( $Q_n > 100 \text{ keV}$ ) transitions and larger for the transitions having lower  $Q$  values ( $Q_n < 100 \text{ keV}$ ), compared to those at  $n_e = 10^{26} \text{ cm}^{-3}$ . However, the total bound state decay contribution to total decay rate decreases slightly with increasing density, at a fixed temperature for all nuclei considered here.

### 5. Total $\beta^-$ decay rate $\lambda_{\text{bare}(s)}$ of bare atom

In the case of bare atoms, the total  $\beta^-$  decay rate is the sum of total bound state decay rate ( $\lambda_b$ ) and total continuum state decay rate ( $\lambda_c$ ). In Table VIII, we show the calculated total decay rate and half-life of the nuclei. In an earlier work, Cosner and Truran [38] calculated total  $\beta^-$  decay rate for the  $s$ -process nuclei without contribution from bound state decay. Takahashi and Yokoi [5] tabulated the total  $\beta^-$  decay rate for highly ionized  $s$ -process nuclei, with bound state decay contribution. However, they did not mention whether these rates include decay of bare atoms. In Table VIII, we show the earlier results of Refs. [5,38] for comparison. Here, the ratio of the calculated half-life of a neutral atom in the terrestrial environment and the half-life of a bare atom in a stellar environment is denoted by  $R$ . The value of  $R$  shows that most of

the bare atoms are short lived compared to the corresponding neutral atoms in the terrestrial environment. This is because of the opening of the  $\beta^-$  decay channel to the atomic bound states from nuclear ground and/or isomeric states and opening of both bound and continuum state decays from the nuclear excited states. However, there are some more deciding factors, which are also reflected in a few exceptional cases, where  $R$  is almost equal to or less than 1.

For the case of  $^{61}\text{Co}$  and  $^{70}\text{Ga}$ , the value of  $R$  is  $\approx 1$ , which implies that for these nuclei the half-lives are almost unchanged. However, in the cases of  $^{66}\text{Cu}$ ,  $^{75}\text{Ge}$ , and  $^{81}\text{Se}$ ,  $R < 1$  in different temperature-density combinations. This indicates that the half-life of a bare atom in the stellar site will be larger than that of a neutral atom in terrestrial conditions. In these cases the competing factors are the inclusion of  $\beta^-$  decay from nuclear excited levels, the increase in the  $\beta^-$  decay rate to the continuum at higher temperature due to the factor  $(1 - f_{FD}(\eta, \beta))$  in Eq. (2), and the effect of continuum depression.

Moreover, from Table VIII, the general trend of  $R$  shows that, with the constant density, increasing temperature results in half-life reduction, except for  $^{66}\text{Cu}$ ,  $^{75}\text{Ge}$ , and  $^{81}\text{Se}$ , whereas for a constant temperature, an increase in density results in an enhancement of the half-life of the bare atom.

## IV. CONCLUSION

In summary, in this study, at first we calculated, using shell model, the comparative half-lives ( $ft$ ) for all allowed terrestrial  $\beta^-$  transitions in the chosen set of nuclei in the mass range  $A = 59-81$ . For this, we used various Hamiltonians



TABLE VII. Variation of bound state  $\beta^-$  decay contribution (in %) for individual transition and to the total decay, with free electron density at a temperature. Columns 5 and 7, bound state  $\beta^-$  decay contribution (%) in individual transition. Columns 6 and 8, contribution (%) to total decay rate from bound state decay. See text for more details.

				$T = 3 \times 10^8 \text{ K}$			
				$n_e = 1 \times 10^{26} \text{ cm}^{-3}$		$n_e = 1 \times 10^{27} \text{ cm}^{-3}$	
Transition details				Bound state decay contribution (%) in individual transition	Bound state decay contribution (%) in total $\beta^-$ decay	Bound state decay contribution (%) in individual transition	Bound state decay contribution (%) in total $\beta^-$ decay
Decay	$J_p^\pi$	$J_d^\pi$	$Q_n(\text{keV})$				
$^{59}\text{Fe} \rightarrow ^{59}\text{Co}$	$3/2_1^-$	$3/2_1^-$	465.7	8.02	12.36	7.83	12.11
		$3/2_2^-$	273.4	15.94		15.67	
		$1/2_1^-$	130.7	33.90		33.75	
$^{60}\text{Co} \rightarrow ^{60}\text{Ni}$	$5_1^+$	$5/2_1^-$	83.4	48.32		48.46	
		$4_1^+$	317.047	14.32	2.18	14.05	2.11
		$2_1^+$	1549.19	1.12		1.08	
		$2_2^+$	723.09	4.46		4.34	
$^{61}\text{Co} \rightarrow ^{61}\text{Ni}$	$7/2_1^-$	$4_1^+$	594.247	6.07		5.91	
		$3_1^+$	473.94	8.45		8.25	
		$5/2_1^-$	1256.4	1.69	1.83	1.63	1.77
		$5/2_2^-$	415.19	10.27		9.91	
		$7/2_1^-$	1320.8	10.57		10.20	
$^{63}\text{Ni} \rightarrow ^{63}\text{Cu}$	$1/2_1^-$	$7/2_2^-$	308.56	14.99		14.53	
		$5/2_3^-$	191.46	25.39		24.84	
		$3/2_1^-$	66.945	60.36	35.45	60.76	35.20
$^{65}\text{Ni} \rightarrow ^{65}\text{Cu}$	$5/2_1^-$	$5/2_1^-$	154.095	32.71		32.50	
		$3/2_1^-$	222.495	22.85		22.56	
		$3/2_1^-$	2137.9	0.62	1.19	0.60	1.14
		$5/2_1^-$	1022.3	2.68		2.60	
		$7/2_1^-$	656.1	5.63		5.48	
		$5/2_2^-$	514.5	8.09		7.90	
		$3/2_2^-$	2132.9	10.96		10.73	
		$7/2_2^-$	43.56	74.52		75.29	
		$5/2_3^-$	30.5	84.42		85.35	
		$1/2_1^-$	$3/2_1^-$	2201.27	0.58		0.56
$^{66}\text{Ni} \rightarrow ^{66}\text{Cu}$	$0_1^+$	$1/2_1^-$	1430.63	1.42		1.38	
		$3/2_2^-$	476.27	9.03		8.82	
		$1_1^+$	251.9	19.99	19.99	19.69	19.69
$^{64}\text{Cu} \rightarrow ^{64}\text{Zn}$	$1_1^+$	$0_1^+$	579.6	7.31	7.31	7.12	7.12
$^{66}\text{Cu} \rightarrow ^{66}\text{Zn}$	$1_1^+$	$0_1^+$	2640.9	0.42	0.61	0.41	0.59
		$2_1^+$	1601.7	1.23		1.19	
		$2_2^+$	768.7	4.72		4.59	
		$0_2^+$	269.2	19.79		19.49	
$^{67}\text{Cu} \rightarrow ^{67}\text{Zn}$	$3/2_1^-$	$5/2_1^-$	561.7	7.65	10.77	7.46	10.52
		$1/2_1^-$	468.4	9.91		9.68	
		$3/2_1^-$	377.1	13.20		12.93	
		$3/2_2^-$	168.2	31.85		31.61	
$^{69}\text{Zn} \rightarrow ^{69}\text{Ga}$	$1/2_1^-$	$3/2_1^-$	910.2	3.82	3.82	3.71	3.72
		$1/2_1^-$	591.8	7.72		7.40	
		$3/2_2^-$	38.5	81.86		82.43	
$^{72}\text{Zn} \rightarrow ^{72}\text{Ga}$	$0_1^+$	$0_1^+$	323.6	16.96	19.99	16.66	19.68
		$1_1^+$	314.3	17.55		17.25	
		$1_2^+$	281.7	19.90		19.59	
		$1_3^+$	234.9	24.23		23.92	

TABLE VII. (Continued.)

				$T = 3 \times 10^8 \text{ K}$			
				$n_e = 1 \times 10^{26} \text{ cm}^{-3}$		$n_e = 1 \times 10^{27} \text{ cm}^{-3}$	
Transition details				Bound state decay contribution (%) in individual transition	Bound state decay contribution (%) in total $\beta^-$ decay	Bound state decay contribution (%) in individual transition	Bound state decay contribution (%) in total $\beta^-$ decay
Decay	$J_p^\pi$	$J_d^\pi$	$Q_n(\text{keV})$				
$^{70}\text{Ga} \rightarrow ^{70}\text{Ge}$	$1_1^+$	$0_1^+$	1651.7	1.35	1.57	1.31	1.52
		$2_1^+$	612.2	7.72	7.52		
		$0_2^+$	436.1	12.41	12.15		
$^{75}\text{Ge} \rightarrow ^{75}\text{As}$	$1/2_1^-$	$3/2_1^-$	1177.2	2.79	3.22	2.71	3.12
		$1/2_1^-$	978.594	3.88	3.77		
		$3/2_2^-$	912.542	4.37	4.25		
		$1/2_2^-$	708.46	6.59	6.42		
		$1/2_3^-$	592.2	8.64	8.43		
		$3/2_3^-$	559.52	9.37	9.15		
		$3/2_4^-$	311.8	19.83	19.52		
		$3/2_5^-$	113.9	49.81	49.90		
		$3/2_6^-$	102.7	53.43	53.61		
		$1/2_4^-$	50.2	77.25	78.06		
		$1/2_5^-$	5.2	100.00	100.00		
	$7/2_1^+$	$9/2_1^+$	1012.97	3.65	3.55		
		$5/2_1^+$	916.232	4.34	4.22		
		$5/2_2^+$	236.09	26.75	26.45		
		$5/2_3^+$	216.69	29.12	28.84		
		$9/2_2^+$	55.88	74.02	74.75		
		$5/2_4^+$	14.59	98.26	98.76		
	$3/2_1^-$	$3/2_1^-$	1430.35	1.93	1.87		
		$1/2_1^-$	1231.74	2.56	2.49		
		$3/2_2^-$	1165.69	2.84	2.76		
		$5/2_1^-$	1150.81	2.91	2.82		
$1/2_2^-$		961.61	4.00	3.88			
$5/2_2^-$		857.94	4.85	4.71			
$1/2_3^-$		845.35	4.97	4.83			
$3/2_3^-$		812.67	5.30	5.16			
$3/2_4^-$		564.95	9.24	9.03			
$3/2_5^-$		367.05	16.36	16.07			
$3/2_6^-$		355.85	16.99	16.69			
$1/2_4^-$		303.35	20.46	20.15			
$1/2_5^-$		258.35	24.37	24.06			
$3/2_7^-$		226.85	27.84	27.55			
$^{78}\text{Ge} \rightarrow ^{78}\text{As}$	$0_1^+$	$3/2_8^-$	80.95	61.76	62.17		
		$3/2_9^-$	59.55	72.02	72.71		
		$5/2_3^-$	10.15	99.57	99.79		
$^{81}\text{Se} \rightarrow ^{81}\text{Br}$	$1/2_1^-$	$1_1^+$	677.7	7.06	10.24	6.88	10.00
		$1_2^+$	661.1	7.33	7.15		
		$1_3^+$	419	13.88	13.59		
$1/2_1^-$	$3/2_1^-$	1585.3	1.81	1.87	1.75	1.81	
	$1/2_1^-$	1047.1	3.92	3.81			
	$3/2_2^-$	1019.26	4.11	4.00			
	$3/2_3^-$	935.4	4.77	4.63			
	$3/2_4^-$	757.01	6.73	6.55			
	$1/2_2^-$	480	13.02	12.74			
	$3/2_5^-$	318.9	21.46	21.12			
	$3/2_6^-$	49.4	80.81	81.55			
$3/2_7^-$	42.1	84.89	85.68				

TABLE VIII. Total  $\beta^-$  decay rate ( $\lambda_{\text{bare}(s)}$  in  $\text{s}^{-1}$ ) and half-life ( $T_{1/2(\text{bare}(s))}$ ) of bare atoms for different density-temperature combinations and comparison with previous results (CT [38] and TY [5]). Half-life of a nucleus is given in units of minutes (min), hours (hr), days (d), and years (yr). Here,  $T_1$  stands for temperature  $T = 1 \times 10^8$  K,  $T_3$  for  $T = 3 \times 10^8$  K, and  $T_5$  for  $T = 5 \times 10^8$  K.  $R$  is the ratio of calculated neutral atom terrestrial half-life to bare atom stellar half-life, i.e.,  $R = T_{1/2(t)}/T_{1/2(\text{bare}(s))}$ . See text for details.

Decay	This work						Previous results	
	$n_e = 1 \times 10^{26} \text{ cm}^{-3}$			$n_e = 1 \times 10^{27} \text{ cm}^{-3}$			$n_e = 1 \times 10^{27} \text{ cm}^{-3}$	$n_e = 1 \times 10^{26} \text{ cm}^{-3}$
	$\lambda_{\text{bare}(s)}$	$T_{1/2(\text{bare}(s))}$	$R$	$\lambda_{\text{bare}(s)}$	$T_{1/2(\text{bare}(s))}$	$R$	$\lambda_{\text{bare}(s)}(CT)$	$\lambda_{\text{bare}(s)}(TY)$
$^{59}\text{Fe} \rightarrow ^{59}\text{Co}$	$T_1$	$2.13 \times 10^{-7}$	37.65 d	1.095	$2.08 \times 10^{-7}$	38.59 d	1.068	$1.80 \times 10^{-7}$
	$T_3$	$2.14 \times 10^{-7}$	37.55d	1.097	$2.10 \times 10^{-7}$	38.21 d	1.079	
	$T_5$	$2.31 \times 10^{-7}$	34.71 d	1.187	$2.28 \times 10^{-7}$	35.19 d	1.171	
$^{60}\text{Co} \rightarrow ^{60}\text{Ni}$	$T_1$	$8.50 \times 10^{-9}$	943.21 d	1.271 <sup>a</sup>	$8.25 \times 10^{-9}$	971.70d	1.234 <sup>a</sup>	$1.30 \times 10^{-8}$
	$T_3$	$1.03 \times 10^{-7}$	78.22 d	15.324 <sup>a</sup>	$1.02 \times 10^{-7}$	78.59 d	15.253 <sup>a</sup>	
	$T_5$	$2.37 \times 10^{-7}$	33.82 d	35.448 <sup>a</sup>	$2.36 \times 10^{-7}$	33.93 d	35.327 <sup>a</sup>	
$^{61}\text{Co} \rightarrow ^{61}\text{Ni}$	$T_1$	$1.03 \times 10^{-4}$	1.86 hr	1.005	$1.03 \times 10^{-4}$	1.87 hr	0.999	$1.17 \times 10^{-4}$
	$T_3$	$1.03 \times 10^{-4}$	1.86 hr	1.006	$1.03 \times 10^{-4}$	1.87 hr	1.001	
	$T_5$	$1.03 \times 10^{-4}$	1.86 hr	1.006	$1.03 \times 10^{-4}$	1.87 hr	1.002	
$^{63}\text{Ni} \rightarrow ^{63}\text{Cu}$	$T_1$	$1.01 \times 10^{-9}$	21.75 yr	2.055	$9.25 \times 10^{-10}$	23.75 yr	1.881	$2.20 \times 10^{-8}$
	$T_3$	$5.17 \times 10^{-9}$	4.25 yr	10.515	$4.97 \times 10^{-9}$	4.42 yr	10.118	
	$T_5$	$1.96 \times 10^{-8}$	1.12 yr	39.812	$1.90 \times 10^{-8}$	1.15 yr	38.742	
$^{65}\text{Ni} \rightarrow ^{65}\text{Cu}$	$T_1$	$7.41 \times 10^{-5}$	2.60 hr	1.026	$7.36 \times 10^{-5}$	2.65 hr	1.019	$7.64 \times 10^{-5}$
	$T_3$	$2.23 \times 10^{-4}$	51.74 min	3.093	$2.23 \times 10^{-4}$	51.91 min	3.083	
	$T_5$	$4.56 \times 10^{-4}$	25.31 min	6.321	$4.55 \times 10^{-4}$	25.37 min	6.307	
$^{66}\text{Ni} \rightarrow ^{66}\text{Cu}$	$T_1$	$3.91 \times 10^{-6}$	49.25 hr	1.177	$3.78 \times 10^{-6}$	50.98 hr	1.137	$3.51 \times 10^{-6}$
	$T_3$	$3.92 \times 10^{-6}$	49.07 hr	1.181	$3.83 \times 10^{-6}$	50.28 hr	1.153	
	$T_5$	$3.93 \times 10^{-6}$	49.00 hr	1.183	$3.85 \times 10^{-6}$	50.03 hr	1.159	
$^{64}\text{Cu} \rightarrow ^{64}\text{Zn}$	$T_1$	$5.42 \times 10^{-6}$	35.54 hr	1.049	$5.34 \times 10^{-6}$	36.08 hr	1.033	$1.20 \times 10^{-5}$
	$T_3$	$5.43 \times 10^{-6}$	35.48 hr	1.050	$5.37 \times 10^{-6}$	35.87 hr	1.039	
	$T_5$	$5.43 \times 10^{-6}$	35.46 hr	1.051	$5.38 \times 10^{-6}$	35.79 hr	1.041	
$^{66}\text{Cu} \rightarrow ^{66}\text{Zn}$	$T_1$	$1.55 \times 10^{-3}$	7.45 min	0.996	$1.55 \times 10^{-3}$	7.47 min	0.993	$2.27 \times 10^{-3}$
	$T_3$	$1.55 \times 10^{-3}$	7.45 min	0.995	$1.55 \times 10^{-3}$	7.47 min	0.993	
	$T_5$	$1.52 \times 10^{-3}$	7.61 min	0.975	$1.52 \times 10^{-3}$	7.62 min	0.973	
$^{67}\text{Cu} \rightarrow ^{67}\text{Zn}$	$T_1$	$3.03 \times 10^{-6}$	63.52 hr	1.080	$2.97 \times 10^{-6}$	64.81 hr	1.059	$3.11 \times 10^{-6}$
	$T_3$	$3.04 \times 10^{-6}$	63.37 hr	1.083	$2.99 \times 10^{-6}$	64.31 hr	1.067	
	$T_5$	$3.04 \times 10^{-6}$	63.32 hr	1.084	$3.00 \times 10^{-6}$	64.11 hr	1.070	
$^{69}\text{Zn} \rightarrow ^{69}\text{Ga}$	$T_1$	$2.19 \times 10^{-4}$	52.74 min	1.020	$2.17 \times 10^{-4}$	53.24 min	1.010	$2.06 \times 10^{-4}$
	$T_3$	$2.19 \times 10^{-4}$	52.68 min	1.021	$2.18 \times 10^{-4}$	53.04 min	1.014	
	$T_5$	$2.19 \times 10^{-4}$	52.65 min	1.021	$2.18 \times 10^{-4}$	52.96 min	1.015	
$^{72}\text{Zn} \rightarrow ^{72}\text{Ga}$	$T_1$	$6.81 \times 10^{-6}$	28.26 hr	1.931	$6.59 \times 10^{-6}$	29.19 hr	1.869	$4.14 \times 10^{-6}$
	$T_3$	$6.83 \times 10^{-6}$	28.17 hr	1.937	$6.68 \times 10^{-6}$	28.83 hr	1.892	
	$T_5$	$6.84 \times 10^{-6}$	28.13 hr	1.940	$6.71 \times 10^{-6}$	28.69 hr	1.902	
$^{70}\text{Ga} \rightarrow ^{70}\text{Ge}$	$T_1$	$5.49 \times 10^{-4}$	21.03 min	1.004	$5.46 \times 10^{-4}$	21.14 min	0.998	$5.46 \times 10^{-4}$
	$T_3$	$5.50 \times 10^{-4}$	21.01 min	1.004	$5.48 \times 10^{-4}$	21.10 min	1.000	
	$T_5$	$5.50 \times 10^{-4}$	21.01 min	1.004	$5.48 \times 10^{-4}$	21.08 min	1.001	
$^{75}\text{Ge} \rightarrow ^{75}\text{As}$	$T_1$	$1.49 \times 10^{-4}$	1.29 hr	1.014 <sup>a</sup>	$1.48 \times 10^{-4}$	1.30 hr	1.006 <sup>a</sup>	$1.40 \times 10^{-4}$
	$T_3$	$1.46 \times 10^{-4}$	1.32 hr	0.994 <sup>a</sup>	$1.45 \times 10^{-4}$	1.33 hr	0.988 <sup>a</sup>	
	$T_5$	$1.20 \times 10^{-4}$	1.59 hr	0.816 <sup>a</sup>	$1.20 \times 10^{-4}$	1.60 hr	0.818 <sup>a</sup>	
$^{78}\text{Ge} \rightarrow ^{78}\text{As}$	$T_1$	$1.43 \times 10^{-4}$	1.34 hr	1.076	$1.41 \times 10^{-4}$	1.37 hr	1.056	$1.33 \times 10^{-4}$
	$T_3$	$1.44 \times 10^{-4}$	1.34 hr	1.078	$1.42 \times 10^{-4}$	1.36 hr	1.063	
	$T_5$	$1.44 \times 10^{-4}$	1.34 hr	1.079	$1.42 \times 10^{-4}$	1.35 hr	1.066	
$^{81}\text{Se} \rightarrow ^{81}\text{Br}$	$T_1$	$5.98 \times 10^{-4}$	19.31 min	1.004 <sup>a</sup>	$5.83 \times 10^{-4}$	19.42 min	0.998 <sup>a</sup>	$6.24 \times 10^{-4}$
	$T_3$	$5.57 \times 10^{-4}$	20.73 min	0.936 <sup>a</sup>	$5.44 \times 10^{-4}$	20.82 min	0.932 <sup>a</sup>	
	$T_5$	$4.37 \times 10^{-4}$	26.43 min	0.734 <sup>a</sup>	$4.35 \times 10^{-4}$	26.53 min	0.731 <sup>a</sup>	

<sup>a</sup>In case of  $^{60}\text{Co}$ ,  $^{75}\text{Ge}$ , and  $^{81}\text{Se}$  the value of R is determined taking the contribution of ground state terrestrial half-life only.

TABLE IX. Details of shell-model calculations: particle partitions used. For fp, single particle state (sps) ordering is  $(1f_{7/2}2p_{3/2}1f_{5/2}2p_{1/2})$ , for fpg, sps ordering is  $(1f_{5/2}2p_{3/2}2p_{1/2}1g_{9/2})$ . In the particle partitions (mentioned in the last two columns) the numbers in the parentheses are minimum and maximum number of particles, respectively, in sps.  $p$ , proton;  $n$ , neutron.

Parent $\rightarrow$ Daughter	Interaction	Code	Formalism	Parent configuration	Daughter configuration
$^{59}\text{Fe} \rightarrow ^{59}\text{Co}$	fpd6	OXBASH	JT	(14, 16), (0, 5), (0, 5), (0, 4);	(14, 16), (0, 5), (0, 5), (0, 4);
$^{60}\text{Co} \rightarrow ^{60}\text{Ni}$	fpd6pn	NUSHELLX	PN	$p$ : (6, 7), (0, 1), (0, 1), (0, 0); $n$ : (7, 8), (3, 4), (0, 2), (0, 1);	$p$ : (6, 8), (0, 2), (0, 0), (0, 2); $n$ : (6, 8), (2, 4), (0, 2), (0, 2);
$^{61}\text{Co} \rightarrow ^{61}\text{Ni}$	fpd6n	OXBASH	JT	(15, 16), (0, 6), (0, 6), (0, 4);	(15, 16), (0, 6), (0, 6), (0, 4);
$^{63}\text{Ni} \rightarrow ^{63}\text{Cu}$	fpd6npn	NUSHELLX	PN	$p$ : (7, 8), (0, 1), (0, 1), (0, 1); $n$ : (8, 8), (0, 4), (0, 6), (0, 2);	$p$ : (8, 8), (0, 0), (1, 1), (0, 0); $n$ : (8, 8), (0, 4), (0, 6), (0, 2);
$^{65}\text{Ni} \rightarrow ^{65}\text{Cu}$	jun45	NUSHELLX	PN	Untruncated	Untruncated
$^{66}\text{Ni} \rightarrow ^{66}\text{Cu}$	fpd6n	OXBASH	JT	(15, 16), (0, 8), (0, 11), (0, 4);	(15, 16), (0, 8), (0, 11), (0, 4)
$^{64}\text{Cu} \rightarrow ^{64}\text{Zn}$	jun45	NUSHELLX	PN	Untruncated	Untruncated
$^{66}\text{Cu} \rightarrow ^{66}\text{Zn}$	jun45	NUSHELLX	PN	Untruncated	Untruncated
$^{67}\text{Cu} \rightarrow ^{67}\text{Zn}$	fpd6n	OXBASH	JT	(15, 16), (0, 8), (0, 12), (0, 4);	(15, 16), (0, 8), (0, 12), (0, 4);
$^{69}\text{Zn} \rightarrow ^{69}\text{Ga}$	fpd6n	OXBASH	JT	(15, 16), (0, 8), (1, 12), (0, 4);	(15, 16), (0, 8), (1, 12), (0, 4);
$^{72}\text{Zn} \rightarrow ^{72}\text{Ga}$	jun45	NUSHELLX	PN	Untruncated	$p$ : (0, 3), (0, 3), (0, 2), (0, 1); $n$ : (0, 6), (0, 4), (0, 2), (0, 10);
$^{70}\text{Ga} \rightarrow ^{70}\text{Ge}$	gx1	OXBASH	JT	(14, 16), (6, 8), (4, 6), (0, 2);	(14, 16), (6, 8), (4, 6), (0, 2);
$^{75}\text{Ge} \rightarrow ^{75}\text{As}$	jun45	NUSHELLX	PN	$p$ : (0, 3), (0, 3), (0, 1), (0, 1); $n$ : (0, 6), (0, 4) (0, 2), (0, 6)	$p$ : (0, 6), (0, 4), (0, 0), (0, 0); $n$ : (0, 6), (0, 4), (0, 2), (0, 10)
$^{78}\text{Ge} \rightarrow ^{78}\text{As}$	jun45	NUSHELLX	PN	$p$ : (0, 6), (0, 4), (0, 1), (0, 1); $n$ : (0, 6), (0, 4), (0, 2), (0, 10);	$p$ : (0, 6), (0, 4), (0, 1), (0, 1); $n$ : (0, 6), (0, 4), (0, 2), (0, 10);
$^{81}\text{Se} \rightarrow ^{81}\text{Br}$	jun45	NUSHELLX	PN	$p$ : (0, 6), (0, 4) (0, 2), (0, 5); $n$ : (0, 6), (0, 4), (0, 2), (0, 10);	$p$ : (0, 6), (0, 4), (0, 2), (0, 0); $n$ : (0, 6), (0, 4), (0, 2), (0, 10)

in fp valance space, and a single interaction in fpg space to reproduce the measured  $ft$  values for different nuclei with empirically obtained GT quenching factors. Only one selected interaction was used to calculate  $\log ft$  values of all transitions in a nucleus. In most of the cases, we found good agreement between the theoretical and the measured  $\log ft$  values. The reliability of the calculated  $\log ft$  for the transitions from the excited nuclear levels is shown. We then compared the calculated terrestrial half-lives with the measured ones. Quite good agreement for most of the cases was found. The presence of bare atoms in the  $s$ -process density-temperature situations

was confirmed by solving the Saha ionization equation, incorporating ionization potential depression. Then we calculated the temperature and density dependence of the individual transition rate and found dependence of the ratio of bound and continuum decay rates on  $Z$  and  $A$  of the daughter. The reason behind it was explained. It is observed that  $\lambda_b$  starts to compete with  $\lambda_c$  and dominates over  $\lambda_c$  for  $Q_m < 100$  keV. We have shown the importance of bound state decay for stellar situations by providing separately the values of  $\lambda_b$  and  $\lambda_c$ . A mild variation of individual transition rate with temperature and density was found. Finally, total stellar  $\beta^-$  decay

rates  $\lambda_{\text{bare}(s)}$  and half-lives  $T_{1/2(\text{bare}(s))}$  as a function of density and temperature were presented. It was noted that for bare atoms, in most of the cases, half-lives become smaller than the terrestrial half-lives of the corresponding neutral atoms. Also, it was found that for some bare atoms, half-lives become larger than the terrestrial ones. These results may be useful for calculations of the nucleosynthesis processes.

### ACKNOWLEDGMENTS

A.G. is appreciative of the financial assistance received from the DST-INSPIRE Fellowship (IF160297). A.G. further expresses gratitude to SERB-DST for providing the computational facility under Government of India Project No. EMR/2016/006339. The author A.G. acknowledges the assistance given by Subham Burai and Sourav Paul at various phases.

### APPENDIX A: SHELL-MODEL CALCULATIONS: CHOICES OF MODEL SPACE AND HAMILTONIAN

We have done shell-model calculations in two valance spaces. The fp model space with  $^{40}\text{Ca}$  core consists of single-particle orbits ( $1f_{7/2}2p_{3/2}1f_{5/2}2p_{1/2}$ ), whereas the fpg model space with  $^{56}\text{Ni}$  core consists of ( $2p_{3/2}1f_{5/2}2p_{1/2}1g_{9/2}$ ) single-particle orbits. Calculations were done with various Hamiltonians available with OXBASH and NUSHELLX for each nucleus to obtain the best theoretical  $\log ft$  values for terrestrial transitions. We reported here, in Table I, only the calculated  $\log ft$  that closely agrees with the corresponding experimental value and the corresponding interaction that was used for that particular nucleus. The description of the details of shell-model calculations with various interactions is shown in Table IX. Some details of the particle partitions used for parent and daughter nuclei are also shown in this table. We used four interaction Hamiltonians, fpd6, fpd6n, jun45, and gx1, as listed in Table IX, either in Isospin (JT) or Proton-Neutron (PN) formalisms. Two formalisms are equivalent. However, we have found some advantages of using the PN formalism while computing with different truncations for protons and neutrons. NUSHELLX admitted larger matrix dimensionalities. The fpd6 interaction is older and quite tested. The interaction jun45 in the fpg valance space was used recently [32] for calculating  $ft$  values in the framework of the shell model. In the following we present in Fig. 9 some of the shell-model results for energy eigenvalues of a few nuclei as representative examples.

### APPENDIX B: SHELL-MODEL CALCULATIONS: QUENCHING FACTOR

The total GT strength (sum rule) measured is in general less than that predicted by shell-model calculation. Hence, theoretically obtained GT transition matrix elements are quenched by a factor  $q$  for agreement with experimental data. The quenching factor is interaction dependent. The method of obtaining the quenching factor is discussed in Sec. III A, and is displayed in Fig. 10 in the case of multiple GT transitions of a parent level to various daughter levels. Each point in these plots represents a single transition, with theoretical  $M(GT)$  value given by the  $x$  coordinate and experimental  $M(GT)$

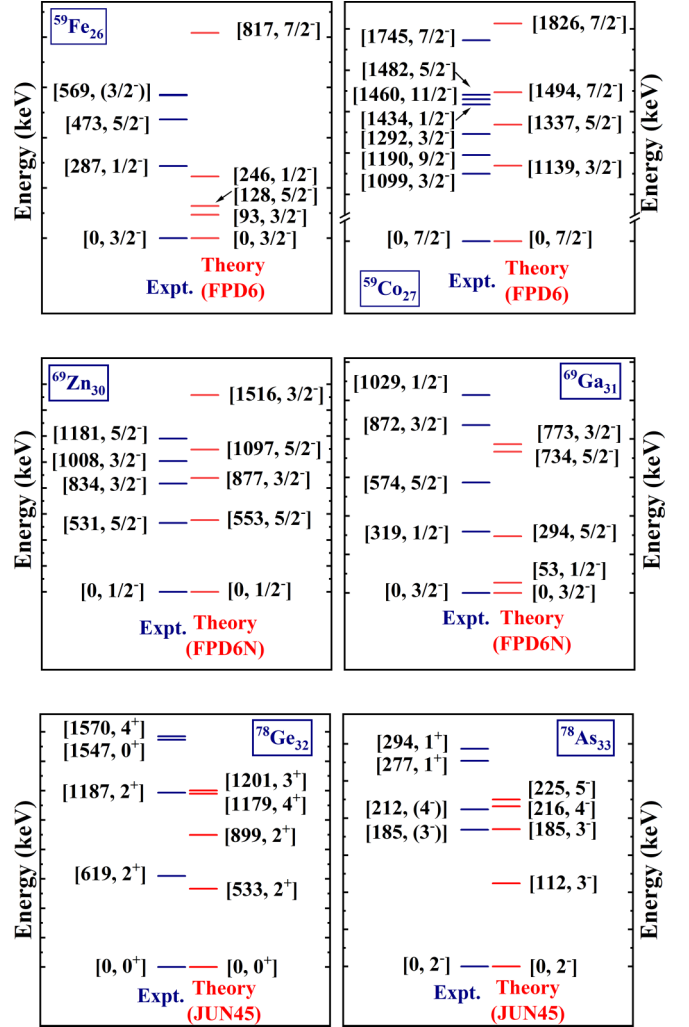


FIG. 9. Comparison between theoretical and experimental level energies. Experimental results are collected from Ref. [19]. Experimental results are rounded off for simplicity. See text for details.

value [19] by the  $y$  coordinate. The dotted lines in these figures are the best fitted line passing through the origin. The slope of the line is the desired quenching factor. The value of the quenching factor for each nucleus is shown in Table I.

### APPENDIX C: SAHA IONIZATION EQUATION

Under local thermodynamic equilibrium (i.e., for specific temperature, free electron density, etc.), the Saha ionization equation provides the fractional population of different ionized states of a particular elemental species as a function of temperature and free electron number density [5]:

$$\frac{n_{ij+1}}{n_{ij}} = \frac{g_{ij+1}}{g_{ij}} \times \left( \frac{M_{ij+1}}{M_{ij}} \right)^{3/2} \times \exp \left( - \frac{(I_{ij} - \Delta_{ij})}{k_B T} - \eta \right), \quad (\text{C1})$$

where the number density of element  $i$  in its  $j$ -times ionized state is expressed as  $n_{ij}$ , atomic partition function as  $g_{ij}$ , mass

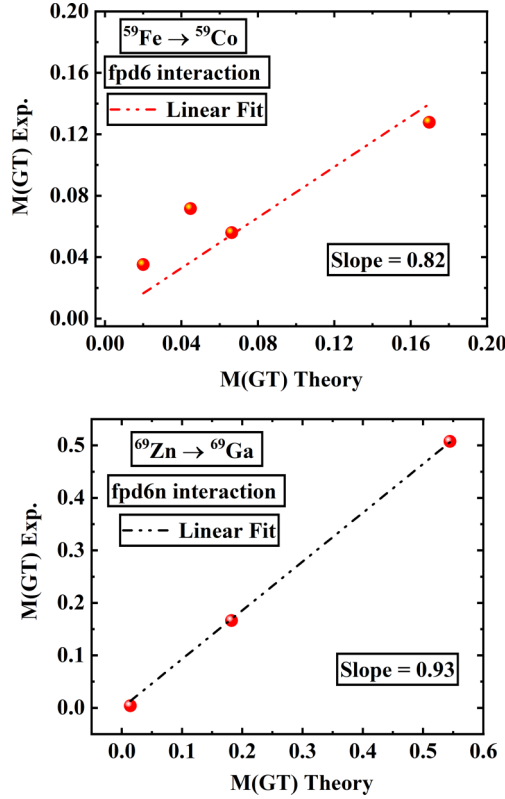


FIG. 10. Theoretical vs experimental  $M(GT)$  to obtain quenching factor. See text for details.

as  $M_{ij}$ , ionization potential depression as  $\Delta_{ij}$  (mentioned as  $\Delta_j$  in the main text), and ionization potential of that state as  $I_{ij}$ .  $k_B$  is the Boltzmann constant and  $T$  is temperature of the stellar site. The parameter  $\eta$  mentioned in the above equation is known as the degeneracy parameter, which can be expressed in terms of free electron density  $n_e$  as

$$F(\eta, b') = n_e \times \pi^2 \times \lambda^3. \quad (\text{C2})$$

Here,  $\lambda = \hbar/m_e c$ ,  $b' = m_e c^2/k_B T$ , and the relativistic Fermi-Dirac integral is given by

$$F(\eta, b') = \int_1^\infty \frac{W \sqrt{W^2 - 1}}{1 + \exp(b'(W - 1) - \eta)} dW. \quad (\text{C3})$$

The total mass density  $\rho$  of a mixture of different elements with mass fraction of the ionized atom,  $x_i$ , satisfies the relationship

$$\rho x_i = \sum_j M_{ij} n_{ij}. \quad (\text{C4})$$

In equilibrium condition, the solution of the Saha ionization equation must satisfy the following relation between total matter density ( $\rho$ ) and free electron number density ( $n_e$ ):

$$\rho \sum_i x_i \frac{\sum_j j n_{ij}}{\sum_j M_{ij} n_{ij}} = n_e. \quad (\text{C5})$$

- [1] D. D. Clayton, *Principles of Stellar Evolution and Nucleosynthesis* (University of Chicago Press, Chicago, 1983).
- [2] R. Daudel, M. Jean, and M. Lecoine, *J. Phys. Radium* **8**, 238 (1947).
- [3] J. N. Bahcall, *Phys. Rev.* **124**, 495 (1961).
- [4] K. Takahashi and K. Yokoi, *Nucl. Phys. A* **404**, 578 (1983).
- [5] K. Takahashi and K. Yokoi, *At. Data Nucl. Data Tables* **36**, 375 (1987).
- [6] B. Budick, *Phys. Rev. Lett.* **51**, 1034 (1983).
- [7] N. C. Nyper and M. R. Harston, *Proc. R. Soc. A* **420**, 277 (1988).
- [8] K. Takahashi, R. N. Boyd, G. J. Mathews, and K. Yokoi, *Phys. Rev. C* **36**, 1522 (1987).
- [9] M. Jung *et al.*, *Phys. Rev. Lett.* **69**, 2164 (1992).
- [10] F. Bosch *et al.*, *Phys. Rev. Lett.* **77**, 5190 (1996).
- [11] K. Yokoi, K. Takahashi, and M. Arnould, *Astron. Astrophys.* **117**, 65 (1983).
- [12] T. Ohtsubo *et al.*, *Phys. Rev. Lett.* **95**, 052501 (2005).
- [13] Yu. A. Litvinov *et al.*, *Rep. Prog. Phys.* **74**, 016301 (2011).
- [14] R. Singh Sidhu, Ph.D. dissertation (2021), <https://archiv.ub.uni-heidelberg.de/volltextserver/30275/>.
- [15] A. Gupta, C. Lahiri, and S. Sarkar, *Phys. Rev. C* **100**, 064313 (2019).
- [16] S. Liu, C. Gao, and C. Xu, *Phys. Rev. C* **104**, 024304 (2021).
- [17] S. Liu and C. Xu, *Chin. Phys. C* **46**, 054106 (2022).
- [18] A. Gupta, C. Lahiri, and S. Sarkar, Poster Presentation at 16th Nuclei in the Cosmos School 2021 (unpublished), [www.jinaweb.org/events/16th-international-symposium-nuclei-cosmos](http://www.jinaweb.org/events/16th-international-symposium-nuclei-cosmos).
- [19] National Nuclear Data Center, <https://www.nndc.bnl.gov/>.
- [20] Atomic Spectra Database, <https://physics.nist.gov>.
- [21] J. C. Stewart and K. D. Pyatt, Jr., *Astrophys. J.* **144**, 1203 (1966).
- [22] E. J. Konopinski and G. E. Uhlenbeck, *Phys. Rev.* **60**, 308 (1941).
- [23] H. Behrens and J. Jänecke, *Numerical Tables for Beta-Decay and Electron Capture* (Springer, Berlin, 1969).
- [24] D. H. Wilkinson, *Nucl. Instrum. Methods Phys. Res., Sect. A* **290**, 509 (1990).
- [25] L. Hayen, N. Severijns, K. Bodek, D. Rozpedzik, and X. Mougeot, *Rev. Mod. Phys.* **90**, 015008 (2018).
- [26] See Supplemental Material at <http://link.aps.org/supplemental/10.1103/PhysRevC.108.015805> for complete beta-decay data, i.e., taking into account the contributions to total decay rate of all excited nuclear levels of parent, for  $^{65}\text{Ni}$ ,  $^{66}\text{Cu}$ ,  $^{75}\text{Ge}$ ,  $^{81}\text{Se}$ , and beta-decay rates with momentum-independent lepton phase space factor.
- [27] H. A. Bethe and E. E. Salpeter, *Quantum Mechanics of One- and Two-Electron Atoms* (Springer-Verlag, Berlin, 1957).
- [28] B. A. Brown and B. H. Wildenthal, *At. Data Nucl. Data Tables* **33**, 347 (1985).
- [29] D. H. Wilkinson, *Nucl. Phys. A* **377**, 474 (1982).
- [30] B. A. Brown *et al.*, MSU-NSCL Report No. 1289, 2004 (unpublished).



- [31] W. D. M. Rae, NUSHELLX, <http://www.garsington.eclipse.co.uk>.
- [32] V. Kumar, P. C. Srivastava, and H. Li, *J. Phys. G: Nucl. Part. Phys.* **43**, 105104 (2016).
- [33] F. Wauters *et al.*, *Phys. Rev. C* **82**, 055502 (2010).
- [34] W. D. Schmidt-Ott, *Z. Phys.* **174**, 206 (1963).
- [35] P. Bhattacharyya *et al.*, *Nuovo Cim. A* **31**, 519 (1976).
- [36] H. T. Easterday, *Phys. Rev.* **91**, 653 (1953).
- [37] A. Kjelberg, E. Hagebø, and R. Nordhagen, *Nucl. Phys. A* **111**, 193 (1968).
- [38] K. Cosner and J. W. Truran, *Astrophys. Space Sci.* **78**, 85 (1981).